SCIENCE CHINA Materials

REVIEWS

mater.scichina.com link.springer.com

Published online 23 June 2016 | doi: 10.1007/s40843-016-5061-1
Sci China Mater 2016, 59(6): 475–494

SPECIAL ISSUE: Flexible and Stretchable Energy

Recent advances and challenges of stretchable supercapacitors based on carbon materials

Xiyue Zhang, Haozhe Zhang, Ziqi Lin, Minghao Yu, Xihong Lu* and Yexiang Tong*

ABSTRACT Stretchable energy storage devices are essential for the development of stretchable electronics that can maintain their electronic performance while sustain large mechanical strain. In this context, stretchable supercapacitors (SSCs) are regarded as one of the most promising power supply in stretchable electronic devices due to their high power densities, fast charge-discharge capability, and modest energy densities. Carbon materials, including carbon nanotubes, graphene, and mesoporous carbon, hold promise as electrode materials for SSCs for their large surface area, excellent electrical, mechanical, and electrochemical properties. Much effort has been devoted to developing stretchable, carbon-based SSCs with different structure/performance characteristics, including conventional planar/textile, wearable fiber-shaped, transparent, and solid-state devices with aesthetic appeal. This review summarizes recent advances towards the development of carbon-based SSCs. Challenges and important directions in this emerging field are also discussed.

Keywords: carbon, stretchable, supercapacitor

INTRODUCTION

Recently, with the development of lightweight, flexible and stretchable materials, advances in materials science and electronics have boomed a nascent field of unconventional electronic devices, such as bending, twisting and stretching [1–5]. As a promising class in demand, it is increasingly more imperative to fabricate and optimize stretchable electronic devices (Figs 1a–g) by changing its rigid materials into one including soft and/or elastic materials for stretchable logic devices [6–8], organic/inorganic light-emitting diode (LED) devices [9], radio frequency devices [10,11], photodetectors [12,13] , field effect transistors [14], pressure and strain sensors [15,16], temperature sensors [17,18], artificial skin sensors [19,20], and bio-inspired devices [21,22]. Since most of the stretchable electronics run on electricity, an indispensable requirement is raised to develop the ideal stretchable energy storage devices that can be integrated and sustain large deformations while maintaining both high mechanical stretchability and excellent electrochemical performance [23–27]. Supercapacitors (SCs) are one kind of the efficient energy storage devices that harness the alternative energy produced and enable the sustainable development of our society [28–30]. It has the advantages of rapid charge/discharge response, simple operating mechanisms, high specific power (Fig. 2a) and long operating life (>100,000 cycles) [31–33]. In this context, stretchable supercapacitors (SSCs), which can sustain large mechanical strain without degradation in their electronic performance, are perceived as one of the most promising power supply in stretchable electronic devices due to their high power density, fast charge-discharge capability and modest energy density [34]. Also, it has a simple device structure with no toxic or inflammable materials, which is safe, durable and relatively facile design [35].

According to the type of the electrode material and the energy storage mechanism, SCs can essentially be classified into three types: [36–38] electrical double-layer capacitors (EDLCs), pseudocapacitors (PCs) and hybrid capacitors in which both the EDLC and PC work together in a single device. The former storage mode is an electrostatic (physical) process in which the electrostatic charge accumulates and separates at the interface between the electrode surface and the electrolyte (Fig. 2b). The latter is a chemical (Faradaic) process with fast and reversible redox reactions between electrode materials and electrolyte ions occurring on the surface of electrodes. In EDLCs, the electrode surface area plays a crucial role in the performance of a capacitor, which can provide higher power densities, fast charge-discharge

School of Chemistry and Chemical Engineering, Sun Yat-Sen University, Guangzhou 510275, China
* Corresponding authors (emails: luxh6@mail.sysu.edu.cn (Lu X); chedhx@mail.sysu.edu.cn (Tong Y))

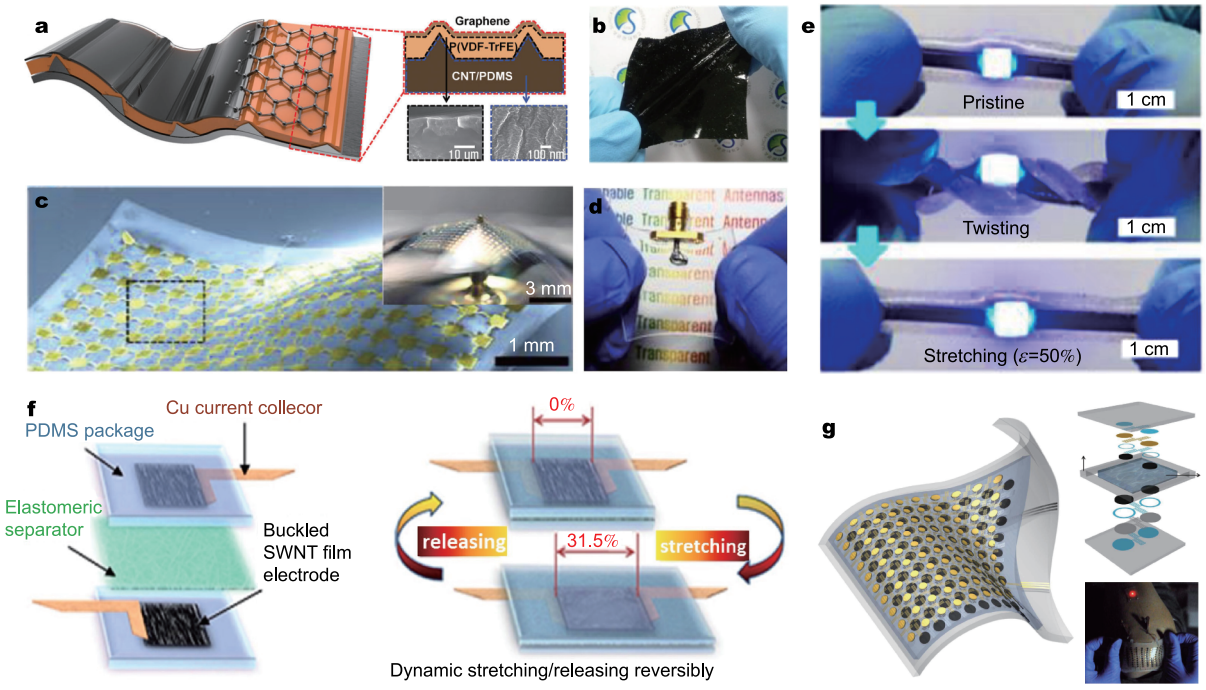

Figure 1 (a, b) Scheme and optical image of a stretchable hybrid nanogenerator. (Reproduced with permission from Ref. [72], Copyright 2014, Wiley). (c) Scheme and optical image of a stretchable logic devices. (Reproduced with permission from Ref. [7], Copyright 2011, American Chemical Society). (d) Optical image of stretchable, transparent radio-frequency antenna. (Reproduced with permission from Ref. [10], Copyright 2016, American Chemical Society). (e) A demonstration of a deformable LED fabricated on the plasticized PEDOT: PSS circuit. (Reproduced with permission from Ref. [14], Copyright 2016, American Chemical Society). (f) Scheme of an SSC. (Reproduced with permission from Ref. [73], Copyright 2012, American Chemical Society). (g) Scheme and optical image of a stretchable lithium-ion battery. (Reproduced with permission from Ref. [27], Copyright 2013, Nature Publishing Group).

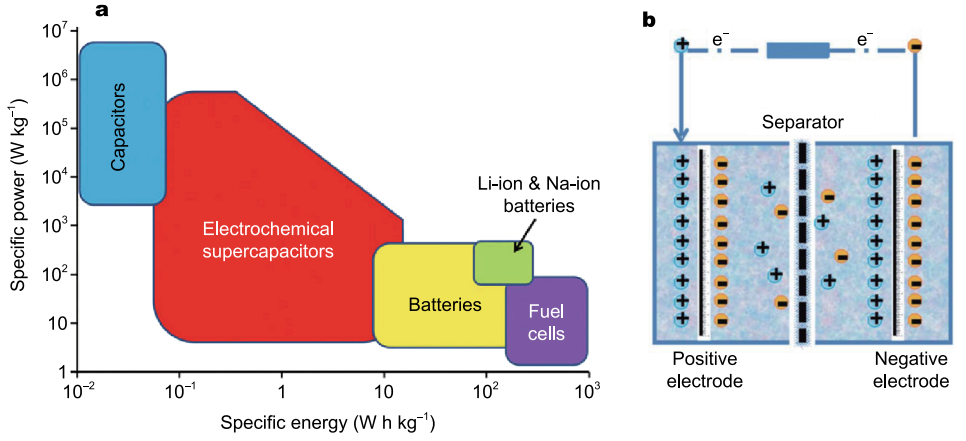

Figure 2. (a) A Ragone plot of various energy storage devices. (Reproduced with permission from Ref. [76], Copyright 2014, Wiley). (b) The scheme of electrical double layer capacitors (EDLCs). (Reproduced with permission from Ref. [77], Copyright 2013, Royal Society of Chemistry).

processes, excellent cycling stabilities, but inferior energy densities. Carbon materials with large specific surface areas and excellent conductivity, such as activated carbon [39,40], carbon nanofibers [41,42], mesoporous carbon [43,44], carbon nanotubes (CNTs) [45,46], graphene [47,48], and carbide-derived carbon [49,50], have been widely employed in EDLCs. While in PCs, composite materials composed of carbon nanomaterials together with electrically conductive polymers (e.g., polyaniline (PANI) [51–54], polypyrrole (PPy) [55–58], and poly[3,4-ethylenedioxythiophene] (PEDOT) [59]) or transition metal oxides (e.g., MnO_2 [60,61], NiO [62,63], RuO_2

[64,65], VO_x [66–68], and TiO_2 [69,70]) have been widely used for the electrodes. PCs, utilizing redox reactions to store/release energy, possess much higher energy densities with compromised power densities [71]. Moreover, conductive polymers usually have a poor cycling life due to the structural instability intrinsically associated with them [74,75]. On the other hand, the limited electrical conductivity and intrinsic rigidity of metal oxides often leads to low power density and poor flexibility. To achieve high electrochemical performance and good mechanical stability for SSCs, therefore, hybrid capacitors could realize further gains if they are used as stretchable power sources.

Earlier studies have demonstrated that carbon materials are promising for the development of SCs in general and flexible SCs in particular, owing to their large surface area, excellent electrical, mechanical, and electrochemical properties. Several recent reviews for SCs based on carbon materials have appeared [78–80], however, recent advances and challenges of carbon-based SSCs has not been tackled in the open literature. The aim of this article is to provide a comprehensive review of various newly-developed SSCs based on carbon materials, including microfilm, sheet, planar-shaped, fiber-shaped, all-solid-state and transparent SCs. We first illustrate CNT-based SSCs with (micro-) film, sheet, planar-shaped and fiber-shaped, followed by synthetic methods of SSCs. Then, we describe graphene-based SSCs and other types of carbon-based SSCs. Finally, strategies to render devices highly stretchable and conductive based on the properties of basic building blocks (substrates, electrolytes and electrodes) will be discussed along with challenges and perspectives in this emerging field.

CNT-BASED STRETCHABLE SUPERCAPACITORS

CNTs possess not only excellent electrochemical performance but also superb mechanical robustness. Owing to their unique porous structures [82], elastic modulus [83], remarkable thermal properties [84], inherent superior conductivity [85], and large specific surface area [86], CNTs or their composites have been extensively investigated as promising electrode materials to make SSCs. Existing SSCs mostly use films or meshes of CNTs as electrodes. The CNTs bridge the mechanical gaps of the metal layer and reduce resistance variations during the stretching process [28]. They will facilitate the charge transfer by providing more channels for electrolyte access and reducing the ion diffusion distance even under mechanical strain. Developed to date, established methods for the preparation of CNTs include laser ablation, arc discharge, and chemical vapor deposition (CVD) [87]. CNTs can be put into mass production at relatively low cost and therefore have attracted widespread academic and industrial interest.

CNT films could buckle and become stretchable via "prestrain-stick-release" approach [88] to assemble SSCs, which consists of three steps: 1) prestraining the elastomeric substrate; 2) transferring the active materials onto the prestrained elastomeric substrate; and 3) releasing the prestrained substrate (Fig. 3a). On this basis, the intrinsically deformable single-walled carbon nanotubes (SWNTs) films are buckled to a periodically sinusoidal pattern (Figs 3b–d). The wavy films after buckling will effectively enhance the interaction with electrolyte and inhibit the decrease of coverage of their active regions that can be realized to withstand the large strain (>30%) generated from large stretching (1%). Several hybrid films can be spread onto the large substrate end to end by this method, which will scale up the area of CNT electrodes and resolve the limitation of CNT film area for large-scale SC electrodes [89].

In a film, where the nanotubes are bundled and entangled together, the conduction of electrons in the film takes place through the bundles as well as by a hopping mechanism where the electrons tunnel from one bundle to another. For the pristine SWNT macrofilm, the resistance (squares in

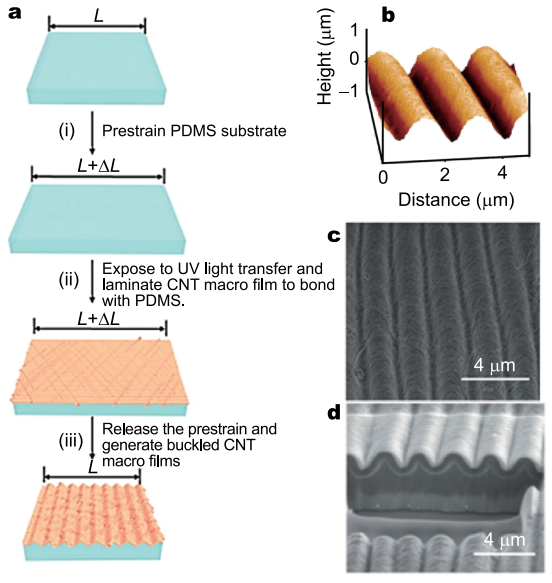

Figure 3 (a) Illustration of the fabrication flow of a buckled SWNT macrofilm comprising surface treatment, transfer, and relaxation of the prestrained PDMS substrate. (b) AFM image of the buckling profile of the SWNT macrofilm. (c) SEM image of a buckled SWNT macrofilm. The buckling wavelength is 2 μm. (d) SEM image of the buckled SWNT macrofilm/PDMS substrate interface. (Reproduced with permission from Ref. [81], Copyright 2009, Wiley).

Fig. 4a) first increases slowly when the tensile strain is less than about 10%, which could be attributed to the combined effects associated with the stretching-induced increase in the active sites of the CNT sheet and loss of the nanotube-nanotube contacts [90]. During the tensile strain and stretch-induced alignment, the overlap length of randomly distributed SWNTs increases and the irreversible elongation of the SWNT macrofilms causes the resistance to increase significantly. Distinguished from the pristine SWNT macrofilms, the electrical resistance of buckled SWNT macrofilms (triangle in Fig. 4a) is also remained while being stretched because the buckled SWNT macrofilms are able to accommodate the applied tensile strains by self-adjusting the wavy pattern's parameters (increasing the wavelength and decreasing the amplitude). By *in situ* electrochemical measurements under dynamic stretching/releasing (DSR) cycles, the electrochemical properties of the SCs remain unchanged with and without 30% uniaxial tensile strain as shown in Fig. 4b. And by various strain rates applied, the fluctuation on the capacitive performance was also observed [73]. Under the DSR mode within ~1% range where the ample time facilitated full access of the ions to the electrode, the diffusion element increased favorably [91,92] (Fig. 4c), but would not significantly affect the electrochemical performance of the cell [74,93,94]. Many studies have demonstrated the feasibility of the buckled SWNT macrofilms to achieve stretchability and meanwhile exhibit excellent electrical conductance, which is critical for SSCs [81].

Due to their ability to sustain large deformation, buckled CNT has higher mechanical properties than CNT films, thus motivated considerable research interest in SSCs. For examples, Yu *et al.* [81] first reported on an SSC based on periodically sinusoidal SWNT macrofilms applied to ultra-

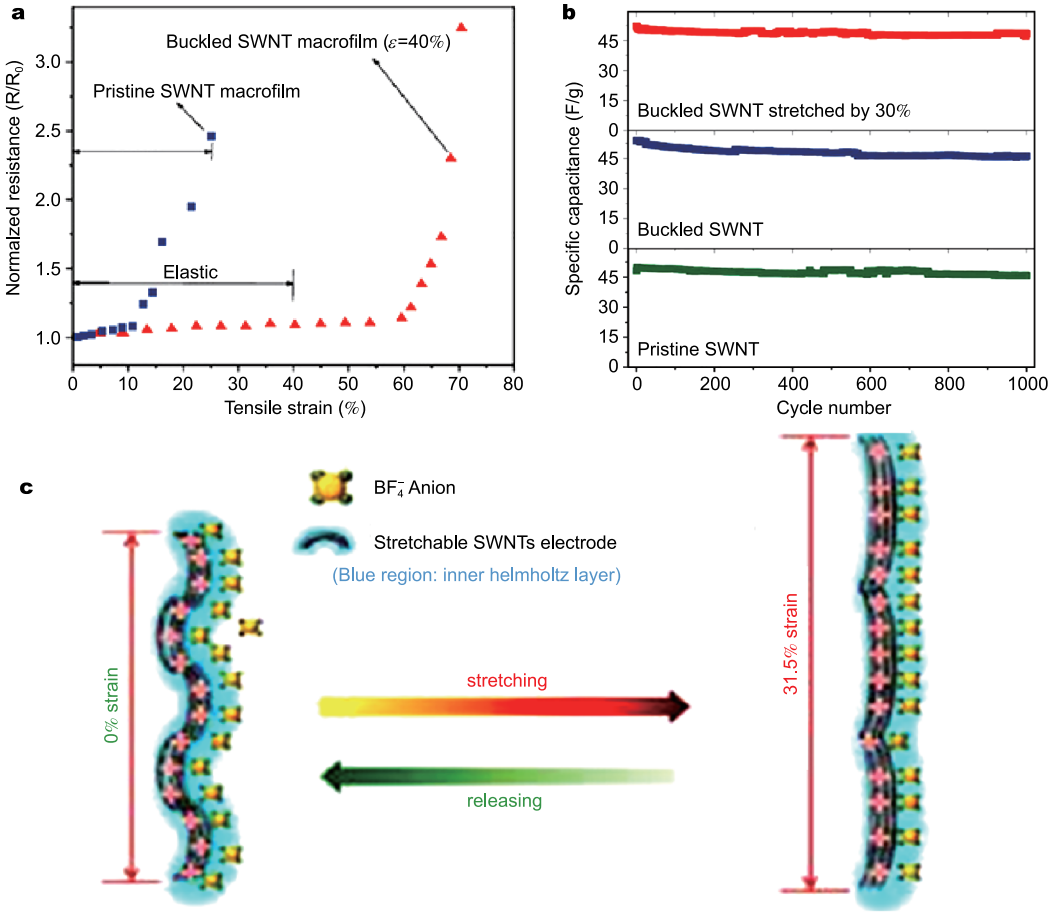

Figure 4 (a) Normalized electrical resistances versus tensile strains of buckled and pristine SWNT macrofilms. (Reproduced with permission from Ref. [81], Copyright 2009, Wiley). (b) Long charge-discharge cycling at 1 A g^{-1} demonstrates the stability of the SSC under 0 and 30% applied tensile strain. (Reproduced with permission from Ref. [81], Copyright 2009, Wiley). (c) Schematic of the stretchable electrode at different strains showing changing electrode/electrolyte interface due to stretching/releasing. (Reproduced with permission from Ref. [73], Copyright 2012, American Chemical Society).

violet (UV) treated PDMS, by using an organic electrolyte, and a non-elastomeric filter paper as separator. The buckled SWNTs-based SSCs showed a maximum specific capacitance of 54 F g^{-1} and a power density of 0.5 kW kg^{-1} with an energy density of 4.2 W h kg^{-1}. Under the application of 30% strain, a specific capacitance value of 52 F g^{-1} was achieved. By changing the separator to electrospun polyurethane (PU) membrane, Li *et al.* [73] demonstrated the buckled SWNTs macrofilms could also stretch up to 30% strain with 50 F g^{-1} of specific capacitance at a scan rate of 100 mV s^{-1}. Nevertheless, the capacitance values for SSCs based on the SWNTs are not capable of reaching their theoretical performance. To further boost their capacitive performance, Jeong *et al.* [95] developed a stretchable electrode using SWNTs spray coated Au modified latex film, which showed good capacitive behavior of 80% retained after stretching to 100% strain, and the highest capacitance value obtained for the un-stretched SWNTs electrode was 119 F g^{-1} in 1 mol L^{-1} Na_2SO_4 at 5 mV s^{-1}. Then they further introduced the reduced graphene oxide (rGO) into SWNTs by ink-jet printing onto PU [96], to reduce the internal resistance and achieve a maximum specific capacitance of 265 F g^{-1} in 1 mol L^{-1} H_2SO_4 at 5 mV s^{-1}.

To compensate for the low energy density, researchers have deposited nanostructured PC materials such as metal oxides and conductive polymers that can enhance the capacity by 200%–300% [97,98].An integrated PC was fabricated by Zhang *et al.* [89] based on free-standing buckled SWCNT/PANI reticulate hybrid films. Taking advantages of π–π stacking interactions between SWCNT and PANI [99,100], both a high specific capacitance of 435 F g^{-1} (for a single electrode) and a high strain tolerance of 140% have been achieved. Gu *et al.* [74] reported the electrochemical performance of buckled MnO_2/CNT hybrid electrodes, with the obtained specific capacitance decreasing to 100 F g^{-1} from about 119 F g^{-1} as the scan rate increases from 50 to 200 mA s^{-1}, and the capacitance retention for the hybrid MnO_2/CNT electrodes dropped to 76.15% and 59% after 10,000 cycles at the strain rates of 3% and 6%, respectively. Furthermore, the outstanding durability is achieved by Tang *et al.* [101] with 96% capacitance retention after 500 cycles at 100% strain. SSC was fabricated by using two electrodeposition prepared CNT/PPy and CNT/MnO_2 films electrodes adhered to two sides of the prestretched hydrogel electrolyte, which reached a specific capacitance of 281.3 F g^{-1} at 2 mA cm^2, and a power density of 519 kW kg^{-1} at an energy density of 40 W h kg^{-1}.

However, in the prestrain-stick-release strategy, the prestraining step might present a challenge for large-scale manufacturing processes. To avoid this prestraining step, Lu and his coworkers [35] have presented a multiwall carbon nanotube (MWCNT) based stretchable film via a facile and large-scale water surface assisted synthesis shown in Figs 5a and b. By combining the excellent conductivity of MWCNTs with the high stretchability of PDMS, numerous CNTs are tangled and form three-dimension (3D)-like network, confirming efficient electron transport through the film which exhibited a high conductivity of 4.19 S cm^{-1} and could be stretched to a high strain of 50% without damaging its conductivity and structure (Fig. 5c). After depositing a layer of PANI nanofibers, the PANI/MWCNT/PDMS film electrode exhibited a benchmark specific capacitance of 1023 F g^{-1} and areal capacitance of 481 mF cm^{-2} at a scan rate of 5 mV s^{-1} (Fig. 5d). The as-fabricated SSCs possessed more than 95% capacitance retention after 500 cycles during the DSR process (Fig. 5e), and delivered a considerably higher maximum energy density of 0.15 mW h cm^{-3} (11 W h kg^{-1}).

Moreover, textiles or papers are directly used as two-dimensional substrates to carry electrochemical active materials [94,102,103]. With a simple "dipping and drying" process using SWNT ink, Hu *et al.* [94] produced highly conductive textiles (Fig. 6a) with conductivity of 125 S cm^{-1} and high specific capacitance of 62 F g^{-1} at a current density of 1 mA cm^{-2}, which was well maintained after being subjected to 100 stretching cycles with 120% elongation. After loading of PPy, the specific capacitance on coated fabric increased to 125.1 F g^{-1} with 60% elongation. Yun *et al.* [104] have further reported PPy-MnO_2-coated CNT textile SC (Fig. 6b), which can reliably operate with high energy (31.1 W h kg^{-1}) and power densities (22.1 kW kg^{-1}) with *in situ* application of both tensile and bending strains. PPy conductive polymer was coated on top of MnO_2 nanoparticles that are deposited on CNT textile SC to prevent delamination of MnO_2 nanoparticles. An increase of 38% in electrochemical energy capacity to 461 F g^{-1} was observed, with the cyclic reliability also improved, as 93.8% of energy capacity was retained over 10,000 cycles (Figs 6c and d). However, the leakage of liquid electrolyte is a risk when those fabricated SCs are integrated into electronic systems. Huang *et al.* [105] designed a new polyelectrolyte comprising polyacrylic acid dual crosslinked by hydrogen bonding and vinyl hybrid silica nanoparticles (VSNPs-PAA). The PPy deposited CNT paper electrodes with a pre-stretched wavy structure connect the broken parts effectively, which contribute to the high electrical conductivity, excellent self-healing property (100% efficiency during all 20 breaking/healing cycles) and stretchability (600%

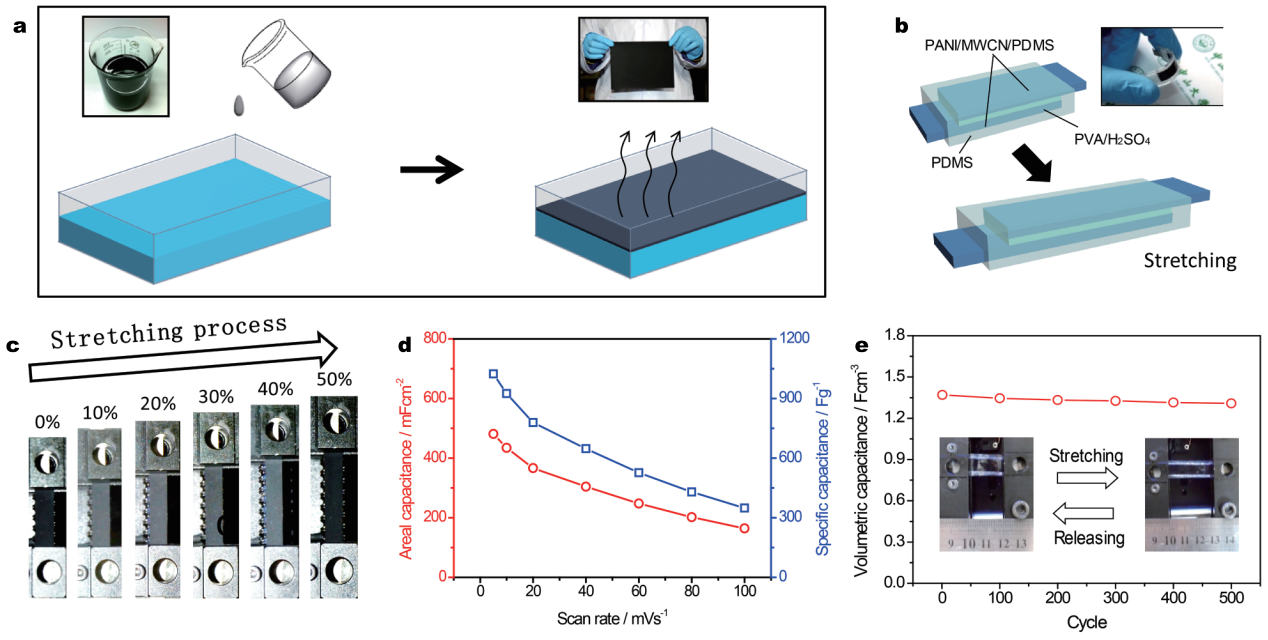

Figure 5 (a) Schematic diagram of fabricating stretchable MWCNT/PDMS film. (b) Schematic diagram of stretchable PANI-SSC. Inset: Digital photograph of a PANI-SSC device. (c) Photographs of the MWCNT/PDMS film containing 10 wt.% MWCNTs with different stains. (d) Areal and specific capacitance as a function of the scan rate of PANI/MWCNT/PDMS electrode. (e) Cycling performance of the PANI-SSC device collected at 10 mV s^{-1} under DSR condition. (Reproduced with permission from Ref. [35], Copyright 2014, Wiley).

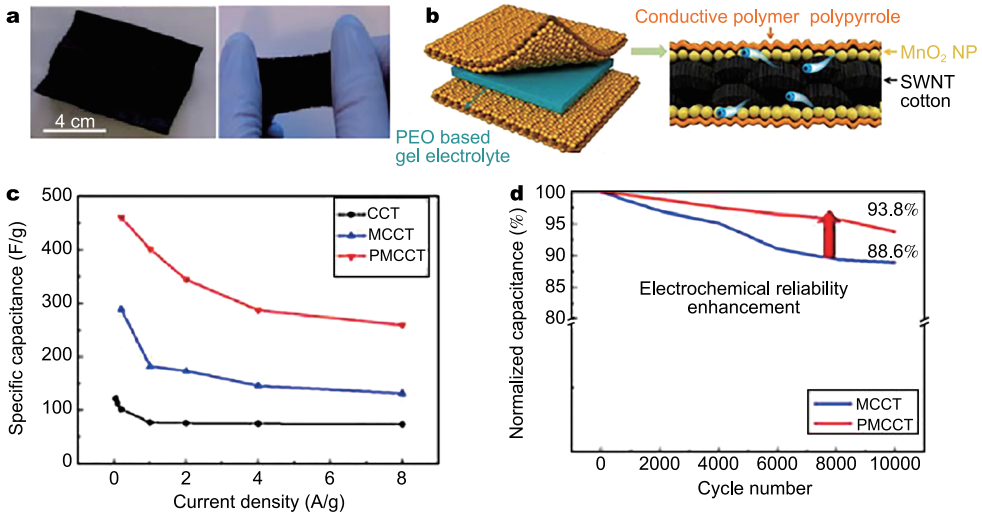

Figure 6 (a) Excellent mechanical properties of conductive textile. (Reproduced with permission from Ref. [94], Copyright 2010, American Chemical Society). (b) Schematic illustration of the fabrication of PPy-MnO_2-coated textile SC. (c) Specific capacitance normalized by the mass for the PPy-MnO_2-coated CNT-textile (PMCCT), MnO_2-coated CNT-textile (MCCT) and CNT-cotton (CCT) electrodes. (d) Electrochemical reliability testing 10,000 cycles for PMCCT and MCCT. (Reproduced with permission from Ref. [104], Copyright 2015, American Chemical Society).

strain with enhanced performance) with the fewest number of components and facile fabrication.

However, the SCs depended on the elasticity materials and the prestrain approaches hindered the integration of SCs into the circuits of stretchable electronics [106]. Huang and his coworkers designed planar-type SCs called a micro-supercapacitor (MSC) [107–109] , capacitance of which can be increased by reducing the path length of ions in the gel electrolyte. They demonstrated a stretchable MSC array interconnected by serpentine metal lines, with planar

spray-coated SWCNT electrodes and an ionic liquid-based triblock copolymer electrolyte [110]. To avoid the possible degradation of the SC upon repeated stretching and releasing, they further fabricated the stretchable MSC arrays on a deformable polymer substrate [106], the strain on the active devices was minimized and all of the strain was accommodated by the soft thin film. With this arrangement, the single and array MSCs exhibit the areal capacitance of 0.63 and 0.57 mF cm^{-2} and maximum volumetric energy densities of 2.6 and 2.4 mW h cm^{-3}, at power densities of 23 and 8 W cm^{-3}, respectively, even under mechanical deformation such as bending, twisting, and uniaxial strain of up to 40%.

In comparison with random CNTs, the aligned CNT sheets offer combined remarkable properties like tensile strength, and excellent optical transmittance [111]. It could be continuously drawn from the spinnable CNT arrays by CVD and easily attached to various substrates to achieve transparent and high electrical conductivities. Due to the decreasing resistance along the aligned direction, the specific capacitance was increased with the increasing thickness of aligned CNT sheets while optical transmittance was decreased [93]. By using two highly aligned CNT sheets as both the current collector and active electrode, Chen *et al.* [90] fabricated a cross-over transparent SSC with a specific capacitance of 7.3 F g^{-1}, which can be biaxially stretched up to 30% strain without any obviously electrochemical change even over hundreds of stretching cycles. By depositing PANI onto aligned CNT sheet electrodes, Peng and his coworkers [93] further developed smart chromatic stretchable capacitors which rapidly and reversibly change colors among yellow, green and blue (Fig. 7a). Due to the improved pseudo-capacitance from the PANI, a specific capacitance of 308.4 F g^{-1} was achieved and well maintained after stretching up to 100% for 200 cycles or bending for 1000 cycles (Figs 7b and c).

As a special kind of SSCs, the SSCs in fiber configuration could be directly weaved into cloth, enabling them to have special application for wearable or on-body electronics. Plenty of attentions were attracted to the fabrication of fiber-shaped SSCs. Recently, to expand the capability of elastic fiber based stretchability, Yang *et al.* [111] demonstrated a fiber-shape SSCs by wrapping aligned CNT sheets on an elastic fiber (Fig. 8a). The high stretchability and specific capacitance (19.2 F g^{-1} at 0.1 A g^{-1}) have been simultaneously achieved by designing a coaxial structure that favors high contact areas between the electrode and electrolyte. And the specific capacitance was further enhanced to 41.4 F g^{-1} by introducing ordered mesoporous carbon components among aligned CNTs in the two electrodes via

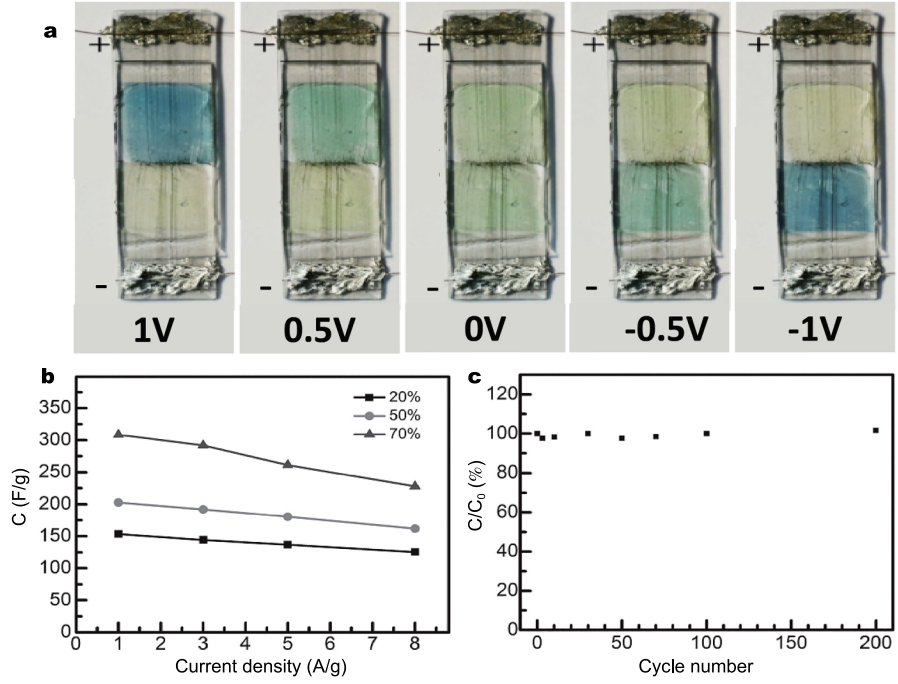

Figure 7 (a) Chromatic transition during a charging-discharging process. (b) Electrochemical characterizations dependence of specific capacitance on PANI weight percentage and current density of the SC. (c) Specific capacitance on stretched cycle number at a strain of 100%. C_0 and C correspond to the specific capacitances before and after stretching. (Reproduced with permission from Ref. [93], Copyright 2014, Wiley).

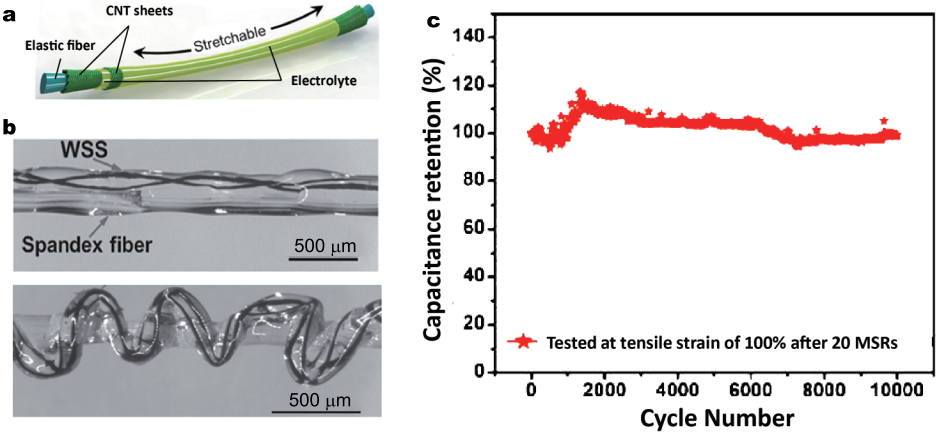

Figure 8 (a) Schematic illustration for the coaxial stretchable wire-shaped SC (WSS) with an elastic fiber. (Reproduced with permission from Ref. [111], Copyright 2013, Wiley). (b) Photographs of straight WSS combined with prestrained spandex fiber and the buckled WSS with relaxed spandex fiber. (c) Cycling performance of the asymmetric SC at current density of 2.8 mA cm^{-2} after 20 mechanical stretching releasing cycles (MSRCs). (Reproduced with permission from Ref. [113], Copyright 2014, Wiley).

dip-coating method. Then, by utilizing the coiling method, the SSCs undergo considerable tensile deformation. Chen *et al.* [112] twisted two such CNT-wrapped elastic wires together to fabricate a fiber-shape SSC, which exhibited an extremely high elasticity of up to 350% strain with a higher device capacitance up to 30.7 F g^{-1} by coating a thin layer of PEDOT/poly(styrene sulfonate) (PEDOT-PSS) onto the electrodes before assembling them into an SC. Xu *et al.* [113] studied an SSC consisting of two undulating CNT fiber electrodes twisted together on a spandex fiber (Fig. 8b), with area specific capacitance of 4.63–4.99 mF cm^{-2}, and the ability to undergo large cyclic tensile strain of 100%. The electromechanical properties of the SC were somewhat improved after 20 mechanical stretching-releasing cycles with the maximum strain of 100% (Fig. 8c). Additionally , Choi *et al.* [114] used a nylon sewing thread that is helically wrapped with a carbon nanotube sheet, and then electrochemically depositing pseudocapacitive MnO_2 nanofibers to achieve the length, area and volume-normalized specific capacitances of 5.4 mF cm^{-1}, 40.9 mF cm^{-2} and 3.8 F cm^{-3} respectively.

However, the introduction of non-capacitive elastomeric polymers increases the volume and weight of the device, showing low specific capacitance and energy density when all the components are taken into account [115]. The construction of lightweight and stretchable power systems without using elastic polymer substrates is critical but remains challenging. Recently, Zhang *et al.* [115] fabricated a free standing SSC by two parallel spring-like CNT fibers and it can withstand tensile strain reaching 100%. These spring-like electrodes can be stretched by over 300%, showing the specific capacitance converted to 0.51 mF cm^{-1} and 27.07 mF cm^{-2} at 150 mA cm^{-3}, with energy densities up to 0.629 mW h cm^{-3} and power densities up to 37.74 mW cm^{-3}. Furthermore, an extremely fiber-shape SSC with a stretchability of up to 350% and a capacitance of 8.0 F g^{-1} at 0.5 A g^{-1} was also reported [112]. Such SCs still suffer from the low capacitance, low working potential (usually 0.8 V), and thus low energy and power densities, preventing them from practical applications. Designing CNTs-based composite electrodes has proven to be an effect strategy to boost the energy storage capacity of fiber-shape SSCs. Xu *et al.* [116] reported a stretchable asymmetric SC with MnO_2/CNT hybrid fiber as the positive electrode and pristine aerogel CNT fiber as the negative electrode, and KOH-PVA gel as electrolyte. The fiber-shape SSC possessed a high specific capacitance of around 157.53 μF cm^{-1} at 50 mV s^{-1} and a high energy density varying from 17.26 to 46.59 nW h cm^{-1} with the corresponding power density changing from 7.63 to 61.55 μW cm^{-1}. Additionally, after 10,000 cycles, the specific capacitance retained over 99%, demonstrating a long cyclic stability. Shang *et al.* [117] further reported a substrate-free, self-stretchable CNT yarn SC based on two twisted CNT yarns consisting of uniformly arranged micro-loops. Under super-elongation (tensile strain up to 150%), arbitrary shape change (entangling), and high frequency stretching (up to 10 Hz over 10,000 cycles), this helical structure can work stably with capacitance retention of 96.6%. And after PPy layer deposition (Fig. 9a), the assembled WSSs boost a specific capacitance from 11.8 to 63.6 F g^{-1} at 100 mV s^{-1}.

Avoiding a high internal resistance in the twisted struc-

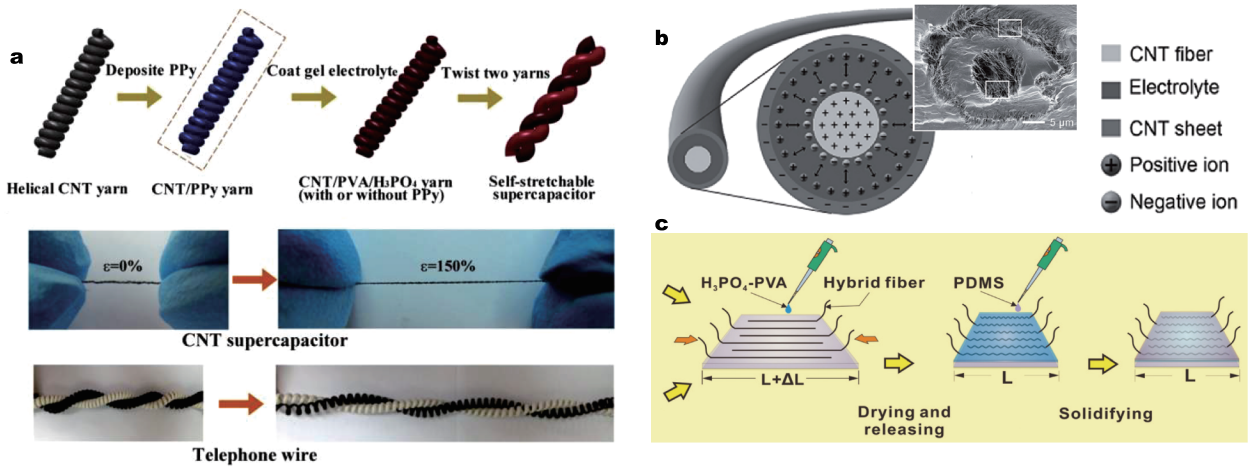

Figure 9 (a) Schematic illustration of the process in which two of CNT yarns were twisted into a double-helix SC and snapshots of a double-helix CNT yarn SC manually stretched to 1.5 times of original length, resembles stretching two telephone wires. (Reproduced with permission from Ref. [117], Copyright 2014, Elsevier). (b) Schematic illustration to both the cross-sectional structure and mechanism for the high electrochemical property of the coaxial EDLC fiber. Insert: SEM images for a cross section. (Reproduced with permission from Ref. [118], Copyright 2013, Wiley). (c) Schematic illustration of the assembly of the omni-directionally SSC. (Reproduced with permission from Ref. [119], Copyright 2015, Royal Society of Chemistry).

ture, the fiber with a coaxial strucrture has fully taken advantage of the large surface area of CNTs also with a much lower internal resistance and high stability. Chen *et al.* [118] have designed and produced a novel family of coaxial EDLC fibers fabricated from a CNT-fiber scrolling by the CNT sheet with a polymer gel sandwiched between them, which can be easily scaled up with high efficiency and low cost (Fig. 9b). This coaxial EDLC fiber exhibited a much higher specific capacitance of 59 F g^{-1} compared with 4.5 F g^{-1} for the twisted structure and power densities up to 755.9 W kg^{-1} at a power density of 1.88 W h kg^{-1}.

However, fiber-based SCs with stretchability along all directions in the plane, like biaxial, have not been reported. Based on porous SWCNT/PEDOT hybrid fiber, Zhang *et al.* [119] designed and fabricated a biaxially SSC, which possesses a unique porous structure both outwardly and inwardly (Fig. 9c). The SC exhibited good transparency, as well as excellent electrochemical properties. Owing to its buckled structure and its fibrous quasi 1D structure, the hybrid fiber manifested a superior capacity of 215 F g^{-1} with 100% stretchability along all directions and stability after being stretched 5000 times.

GRAPHENE-BASED STRETCHABLE SUPERCAPACITORS

Graphene with single-layered two-dimensional sp^2 hybridized carbon sheets has become of central interest due to its unique properties, including large specific surface area, giant electron mobility [120,121], high chemical and thermal stability [122,123], ultrahigh strength [124,125], higher conductivity, ideal electrochemical capacitance [126–128] and excellent optical transparencies [129,130], compared with those of other carbon nanomaterials [131]. In this regard, graphene holds great potential as stretchable electrodes in SSCs.

For instance, 3D interpenetrating graphene electrodes, which allow the access of electrolyte ions to the internal surface of the graphene film thus lowering internal contact resistance compared to CNT network, have been fabricated by electrochemical reduction of GO for ultrahigh rate SCs [132–134]. Li *et al.* [135] fabricated rGO-based SSCs with 3D interdigital electrodes and solid electrolyte multilayers via pressure spray printing and machine coating to achieve high and adjustable volumetric capacitance (77.9 F cm^{-3} with the 5 μm rGO layer), excellent flexibility, and stretchability. By introducing the concept of hybrid electrode, later, Xie *et al.* [136,137] showed that 3D MnO_2/graphene electrode collapsed, and cracked easily during bending or stretching operations due to the intrinsic rigidity of MnO_2. So that Nam *et al.* [138] recently illustrated that deformation can be accomplished using a stretching component like CNT cluster as a motor riding on the graphene track. So a graphene–CNT-layered structure is fabricated for SSCs with a high value of capacitance in the deformed state of 329 F g^{-1} (based on mass of the graphene) without a decrease while stretched up to 80% strain. The interaction and moving motion of the graphene–CNT electrodes are also revealed by first-principle calculations and 3D finite-element methods which can be demonstrated by comparing them to the actin–myosin interaction in muscles. In

addition, the energy density of SCs has been increased by varying the operating voltage and using ionic liquid electrolyte [139]. The higher stability and rate capability of the graphene based SSC are achieved in an ionic liquid incorporated PMMA/[BMIM][TFSI] electrolyte where hydrogen exfoliated graphene has been dispersed as electrode by Tamilarasan *et al.* [140]. In terms of mass of total electrode material, the specific capacitance, energy density and power density of the device was 83 F g^{-1}, 26.1 W h kg^{-1} and 5 kW kg^{-1}, respectively, at the specific current of 2.67 A g^{-1}, with at least 90% capacitance retained under repeated 30% strain cycles.

These modifications show valuable characteristics in enhancing the performance of SSCs, especially with the in-plane structure; however, it still remains a great challenge to optimize the tensile properties of graphene-based stretchable electrodes while maintaining high performance. In contrast, wrinkled structure (Fig. 10a) can release the strain by changing its shape with an out-of-plane bend, even though the electrode materials are stiff. Most recently, a transparent SSC based on CVD-grown wrinkled multilayer graphene electrodes has been reported by Chen *et al.* [141], which is capable of sustaining a tensile strain of up to 40% with transparency up to 60% (at 550 nm) even over hundreds of stretching cycles. The surface-specific capacitances thus calculated for the SCs based on the planar and wrinkled graphene sheets are 4.9 and 5.8 μF cm^{-2}, respectively, while the corresponding mass-specific capacitances are 6.4 and 7.6 F g^{-1}. Moreover, Xu *et al.* [91] demonstrated the implementation of a laminated ultrathin four-layer CVD graphene film transferred and buckled on PDMS substrates as a stretchable (40%) and transparent (72.9% at 550 nm) electrode for SCs. As the tensile strain increased up to 40%, the specific capacitance (5.33 μF cm^{-2} at a scan rate of 200 mV s^{-1}) showed no degradation and even increased slightly. Later, they further investigated the strain variation in buckled four-layer graphene/PDMS films as the applied tensile strain increased from 0 to 40% using atomic force microscopy (AFM) and micro-Raman mapping, which confirmed that the graphene film in the buckled state is suitable for its application as a stretchable electrode [142].

The direct adhesion part between electrode materials and stretchable substrate may limit the stretchability and stability of the devices. The decrease of strain induced into the suspended wavy structure (Fig. 10b) is more remarkable after enlarging the stress applied, as shown in the relevant strain distribution (Fig. 10c) [92]. Assuming that the conductive belt deposited on tripod structure PDMS substrates could prevent the deformation with small curve radius and no direct contact between the conductive metal film and the elastic substrate, they designed suspended wavy graphene microribbons for highly stretchable MSCs which showed a capacitance of 0.54 mF cm^{-2} at a scan rate of 500 mV s^{-1}, and remained nearly unchanged (about 92%) when stretched by 100% for as many as 5000 cycles. Furthermore, the wavy-shaped PANI/graphene electrodes were also used to fabricate the SSC [136], which showed a maximum specific capacitance of 261 F g^{-1} and an energy density of 23.2 W h kg^{-1} at a power density of 399 W kg^{-1} for a 0.8 V voltage window at a maximum strain of 30%.

A novel road is reported for demonstrating practical applications of the crumpled-graphene-paper electrodes [143]. The nano-porous structure graphene paper is attached on an elastomer film that has been uniaxially or biaxially stretched into patterns, so that the graphene paper is folded and crumpled. The results show that this commercial strategy has its unprecedented set of merits

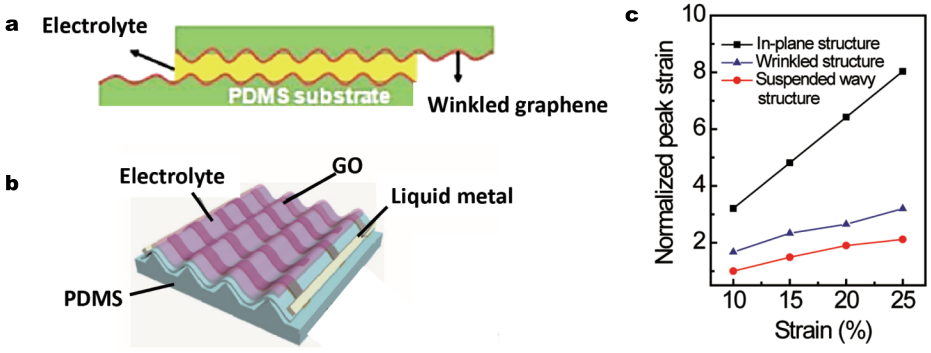

Figure 10 (a) Schematic representation of the SSC fabricated by wrinkled graphene sheets. (Reproduced with permission from Ref. [141], Copyright 2013, American Chemical Society). (b) Schematic drawing of the stretchable MSC onto the tripod-structured PDMS substrate. (c) The peak strain comparison of in-plane structure, wrinkled structure, and suspended wavy structure, respectively. (Reproduced with permission from Ref. [92], Copyright 2015, Wiley).

including low-cost, simple fabrication, extremely high stretchability (e.g., uniaxial strain, 300%, areal strain, 800%), high specific capacitance (e.g., 196 F g^{-1}), and high reliability (e.g., 96% over 1000 stretch/relax cycles).

Graphene fibers (GFs) stands for a new type of fibers of practical importance, which integrate such the common characteristics of fibers like the mechanical flexibility for textiles and unique properties such as low cost, light weight, and ease of functionalization in comparison with conventional carbon fibers [144–146]. And graphene based textile electrodes demonstrated high capacitance and flexibility [147–149]. However, the stretchablility of those textile electrodes was not discussed. The challenge to assemble two-dimensional (2D) microcosmic graphene sheets into macroscopic fibrillary configuration, has been only handled recently [144–146,150]. Therefore, researchers are striving to find feasible method for preparing graphene-based electrodes with satisfactory electrochemical performance, including high volumetric capacitance and long cycle life [151,152], and to further improve the capacitance, metal oxides, and conducting polymer are introduced to composite with carbon materials [153–155].

So far, only a few papers addressed graphene-based stretchable WSSs or textile SCs. Meng *et al.* [156] fabricated a spring-like SC consisting of two all-graphene core sheath fibers twisted together (Fig. 11a) with highly compressible and stretchable properties, which inherits the intrinsic high conductivity and mechanical flexibility of GF in combination with highly exposed surfaces of graphene sheets, thus the resulting SSCs has a specific capacitance of 25–40 F g^{-1} and a power density of 6–100 × 10^{-6} W cm^{-2} at an energy density of 0.4–1.7 × 10^{-7} W h cm^{-2}. Moreover, Zang *et al.* [157] designed a dynamically stretchable solid state SC using graphene woven fabric (GWF) assembled by intersecting graphene micron-ribbons with many grids. PANI was deposited on GWF through *in-situ* electropolymerization to improve the capacitance from 26 μF cm^{-2} (GWF only) to 8 mF cm^{-2} (GWF+PANI). After transferred on pre-stretched PDMS, the SSCs possess excellent static and dynamic stretchability (up to 30%) with excellent galvanic stability even under high strain rates (up to 60% s^{-1}) (Fig. 11b). By utilizing the cost-effective technique, Zhao *et al.* [158] reported SCs fabricated from rGO coated pre-existing nylon lycra fabric electrode via a facile dyeing approach. After the addition of a chemically synthesized PPy, the assembled SC achieves an energy density of 2.53 W h kg^{-1}, and delivers a specific capacitance from 12.3 F g^{-1} to 114 F g^{-1} at a scan rate of 5 mV s^{-1} with an improved cycling stability (89% capacitance retention after 2000 cycles at 50% strain) and a higher capacitance at 50% strain when compared to the performance observed with no strain. By using a representative conducting polymer of PPy as a mediator, Zhao *et al.* [159] developed a unique strategy for *in-situ* formation of PPy-graphene foam hydrogel (Fig. 11c) to achieve a remarkable compression tolerance and demonstrated a high porosity, conductivity, and excellent mechanical strength (50% compressive strain) with the specific capacitances of 350 F g^{-1}. Apart from the contribution to the capacitance performance, the presence of conjugated polymer of PPy could increase the strength of 3D structure via strong π–π interaction to bear a certain extra force and maintain large specific retention under compressive strain of 50% even up to 1000 cycles.

OTHER TYPES OF CARBON-BASED STRSTRETCHABLE SUPERCAPACITORS

Beside CNTs and graphene, carbon fiber has attracted initial studies of SCs [153,161–163]. To demonstrate the application of the carbon fiber thread in stretchable electronics, Jin *et al.* [160] twisted carbon fiber thread/polyaniline (CFT/PANI) and functionalized CFT electrodes together to prepare a solid-state asymmetric fiber-shaped SC (Fig. 12a) with high operating voltage (1.6 V). The as-prepared device shows a volumetric energy density up to 2 mW h cm^{-3}, with the maximum power density of 11 W cm^{-3}, which is comparable to typical commercial SCs. They wound the device onto a conventional elastic thread to form an SSC (Fig. 12b). Other than good rate capability and high volumetric capacitance, the capacitance of the stretchable device is well maintained even after stretching up to 100%, demonstrating its excellent stretchability (Fig. 12c). Table 1 summarizes the electrochemical performance of some representative SSCs.

CONCLUSIONS AND PERSPECTIVES

Undoubtedly, existing carbon-based SSCs electrodes are mostly based on graphene and CNT materials. A large variety of stretchable and even transparent SSCs based on carbon electrodes of different shapes (e.g., planar, wire) with controllable architectures (e.g., aligned, buckled, wavy, foam-like) have been developed. Furthermore, metal oxides (MnO_2), as well as conductive polymers (PANI, PPy, and PEDOT) are two common materials used to enhance the capacity of SSCs by depositing on elastic or carbon coated substrate.

Due to the structural interconnectivities and unique elastic modulus, CNTs possess not only excellent electrochemical performance, but also superb mechanical robustness.

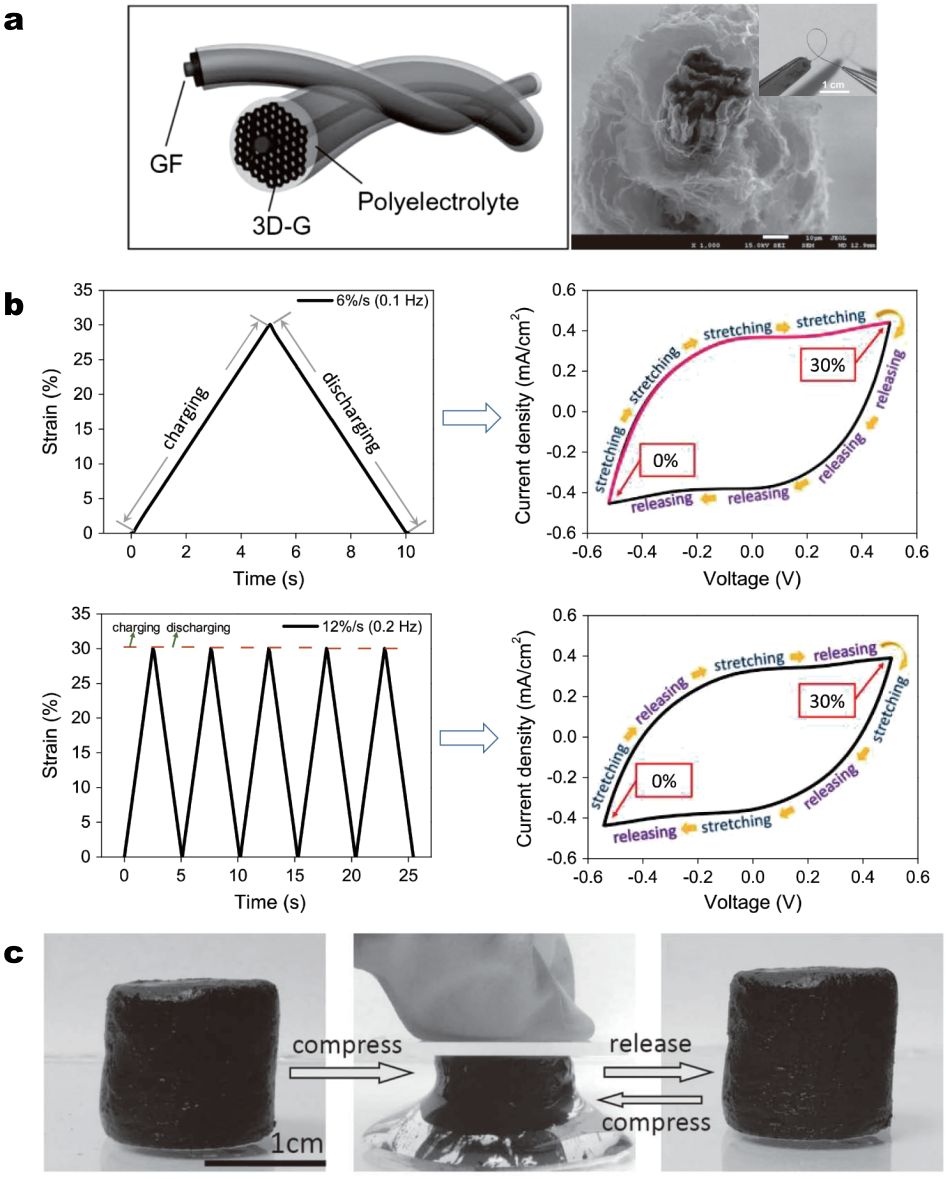

Figure 11 (a) Schematic illustration of a wire-shaped SC fabricated from two twined GF@3D-Gs with polyelectrolyte and SEM imagines of cross-section view of a GF@3D-G. (Reproduced with permission from Ref. [156], Copyright 2013, Wiley). (b) Schematic illustration of stretchable GWF based SC and its dynamic performance under different stretching states (6% s^{-1} and 12% s^{-1}). Strain-time curve (left) and corresponding CV curve (right). (Reproduced with permission from Ref. [157], Copyright 2015, Elsevier). (c) The compression-recovery processes of PPy-G foam. (Reproduced with permission from Ref. [159], Copyright 2013, Wiley).

In this term, CNTs with various structures like buckled film, aligned sheet, twisted/coaxial fiber or yarns have been used for improving the mechanical properties of different devices such as planar, fiber and textile SSCs. However, there are only a few papers addressing graphene-based stretchable WSSs or textile SCs, which is more promising for further development.

As for the fabrication methods, in general, three main strategies are reported to develop SSCs: 1) assembling devices with all stretchable components; 2) connecting stiff active device islands with stretchable linker; 3) obtaining stretchability through waved or textile structure. Owing to their unique and advantageous design for 2D nanomaterials based energy storage devices, planar SCs have attracted much attention with three structures being developed including in-plane, wrinkled/bulked and suspended wavy structure. In addition, these three main strategies were demonstrated to develop SSCs for textile. For in-

Table 1 Comparison of the performance of carbon based SSCs

Electrode	Substrate	Electrolyte	Specific capacitance ($F\ g^{-1}$)	Areal capacitance ($mF\ cm^{-2}$)	Energy density ($W\ h\ kg^{-1}$)	Power density ($kW\ kg^{-1}$)	V (V)	Capacitance retention	Ref.
SWNT	PDMS	Ion-gel	51.8 (at 1 A g^{-1}) 42.8 (at10 A g^{-1})	2.88 2.39	15.7 9.59	1.48 12.7	3.0	96.6% (3000 cycles at 20% strain)	[28]
SWNT	PDMS	Ion-gel	55.3 (at 0.5 V s^{-1}) 34.2 (at 10 V s^{-1})	/	20.7 (at 5 A g^{-1}) 11.5 (at 50 A g^{-1})	7.4 70.5	3.0	99% (10 cycles at 30% strain)	[110]
MWNT	/	Gel	/	27.07 (at 0.15 A cm^{-3})	/	/	1.0	94% (300 cycles at 100% strain)	[115]
SWNTs	Latex rubber	H_2SO_4	119 (at 5 mV s^{-1})	/	33.5	50.3	1.0	80% (100 cycles at 100% strain)	[95]
SWNT	Fabric sheet	$LiPF_6$	62 (at 1 mA cm^{-2})	19.2	20	10	3.0	94% (8000 cycles at 120% strain)	[94]
MWNT	Elastic fibers	Gel	19.2 (at 0.1 A g^{-1})	/	0.515–0.363	19–421	0.8	95% (1000 cycles at 75% strain)	[111]
MWNT	Elastic fibers	Gel	8 (at 0.5 A g^{-1})	/	/	/	0.8	105% (100 cycles at 200% strain)	[112]
Buckled SWNT	PDMS	Organic	54 (at 1 A g^{-1})	/	4.2	0.5	1.5	99% (1000 cycles at 30% strain)	[81]
Buckled SWNT	PDMS	Organic	50 (at 100 mV s^{-1})	2.64 (at 10 A g^{-1})	/	/	1.5	94.6% (2521 cycles at strain rate of 4.46% s^{-1})	[73]
Aligned CNT sheet	PDMS	Gel	7.3 (at 0.25 A g^{-1})	/	2.4	0.9	0.8	170% and 100% (100 cycles at 30% strain of the parallelly and cross assembled)	[90]
CNT fiber / sheet	/	Gel	59 (at 1 μA)	8.66	1.88	0.756	1.0	90.8, 84.6, and 81.6% (25, 50, and 75 cycles at 10% strain)	[118]
Dry/aerogel spun CNT fiber	PDMS	Gel	/	4.42 8.16 (at 50 mV s^{-1})	/	/	0.8	81.4% 121.9% (10,000 cycles at 40% strain)	[164]
CNT fiber	Spandex fiber	Gel	/	4.28 (at 50 mV s^{-1})	0.8–2.26 × 10^{-7} W $h\ cm^{-2}$	4.93 × 10^{-4} W cm^{-2}	0.8	108% (20 cycles of 100% strains)	[113]
CNT/PPy	/	Gel	63.6 (at 100 mV s^{-1})	/	/	/	1.0	96.6% (10,000 cycles at 50% strain)	[117]
CNT/PEDOT	PDMS	Gel	53 (at 1 A g^{-1})	1.6	6	19.2	0.9	96.9% and 90.1% (5000 cycles at 100% strain in the X- and Y-directions)	[119]
CNT/PEDOT-PSS	Elastic fibers	Gel	30.7 (at 0.5 A g^{-1})	/	/	/	0.8	105% (100 cycles at 200% strain)	[112]
CNT/Mn_3O_4	PDMS	Gel	/	0.63 (single) 0.57 (array)	/	/	0.8 3.0	92% (30,000 cycles at 40% strain)	[106]
CNT/MnO_2	/	Hydrogel	201.1 (at 0.5 mA cm^{-2})	478.6	/	/	0.8	91.5% (3000 cycles at 150% strain)	[98]

(*To be continued on the next page*)

(*Continued*)

Electrode	Substrate	Electrolyte	Specific capacitance ($F\ g^{-1}$)	Areal capacitance ($mF\ cm^{-2}$)	Energy density ($W\ h\ kg^{-1}$)	Power density ($kW\ kg^{-1}$)	V (V)	Capacitance retention	Ref.
CNT/MnO_2	PDMS	$TEABF_4$/PC	100 (at 200 $mV\ s^{-1}$)	/	/	/	1.5	76.15% (10,000 cycles at the strain rates of 3%)	[74]
CNT/MnO_2/PPy	/	Hydrogel	281.3 (at 2 $mA\ cm^{-2}$)	281.3	40	519	2.0	96% (500 cycles at 100% strain)	[101]
CNT/PANI	PDMS	Solid	106 (at 1 $A\ g^{-1}$)	/	8.3	20.1	0.75	85% (1000 cycles at 120% strain)	[89]
CNT/PANI/PDMS film		Gel	1023 (at 5 $mV\ s^{-1}$)	481	11	/	0.8	95.6% (500 cycles at 50% strain)	[35]
Aligned CNT/PANI	PDMS	Gel	308.4 (at 8 $A\ g^{-1}$)	/	/	/	1.0	109.4% (200 cycles at 100% strain)	[93]
CNT/MnO_2/PPy	Cotton textile	PEO/Na_2SO_4 gel	461 (at 0.2 $A\ g^{-1}$)	38.3	31.1	22.1	2.4	98.5% (a cycle at 21% strain)	[104]
CNT/MnO_2 fiber	Nylon	Solid	/	40.9 (at 10 $mV\ s^{-1}$)	2.6×10^{-3} $W\ h\ cm^{-2}$	/	1.0	86.5, 90.8, and 87.8% (a cycle of 150% strains of 6, 12, and 17.1% strain/s)	[114]
CNT/PPy	/	Polymer	85 (at 500 $mV\ s^{-1}$)	/	/	/	0.6	220% (a cycle of 600% strains)	[105]
SWNTs/rGO	PU	H_2SO_4	265 (at 5 $mV\ s^{-1}$)	/	/	/	1.0	68.6% (100 cycles at 100% strain)	[96]
SWNTs/graphene	/	Gel	58.4 (at 0.15 $A\ g^{-1}$)	/	/	/	0.8	99% (a cycle at 80% strain)	[138]
Graphene film	PDMS	Gel	17.3 (at 200 $mV\ s^{-1}$)	5.33×10^{-3}	0.27×10^{-9} $W\ h\ cm^{-2}$	11.77×10^{-6} $W\ cm^{-2}$	0.8	98% (10,000 cycles at 40% strain)	[91]
Graphene film	/	Polymer	83 (at 2.67 $A\ g^{-1}$)	/	26.1	5	3	90% (10 cycles at 30% strain)	[140]
rGO film	PP	Gel	140.2 (at 0.01 $A\ g^{-1}$)	/	/	/	1.0	97% (4000 cycles with different ε at 1.0 and 1.3)	[135]
rGO microribbon	PDMS	Gel	/	0.54 (at 500 $mV\ s^{-1}$)	0.52×10^{-3} $W\ h\ cm^{-2}$	0.417 $W\ cm^{-2}$	0.8	92% (5000 cycles at 50% strain)	[92]
Graphene planar or wrinkled sheet	PDMS	Gel	6.4 or 7.6 (at 1.0 $V\ s^{-1}$)	4.9×10^{-3} or 5.8×10^{-3}	/	/	0.8	98% or 100% (100 cycles at 40% strain)	[141]
Crumpled graphene paper	Elastomers	Gel	49 (at 1 $A\ g^{-1}$)	/	30	/	1.0	96% (1000 cycles at 200% strain)	[143]
Graphene fiber	/	Gel	25–40 (at 50 $mV\ s^{-1}$)	1.2–1.7	$0.4–1.7\times10^{-7}$ $W\ h\ cm^{-2}$	$6–100\times10^{-6}$ $W\ cm^{-2}$	0.8	100% (a cycle at 200% strain)	[156]
rGO/PPy	Nylon lycra	Aqueous	114 (at 5 $mV\ s^{-1}$)	/	/	/	0.8	79% (2000 cycles at 50% strain)	[158]
Graphene/PPy foam	/	Aqueous	350 (at 1.5 $A\ g^{-1}$)	/	/	/	1.0	100% (1000 cycles at 50% compressive strain)	[159]
Graphene/PANI	Ecoflex	Gel	261 (at 0.38 $A\ g^{-1}$)	/	23.2	0.399	0.8	95% (100 cycles at 30% strain)	[136]
Carbon fiber/PANI	Elastic thread	Gel	/	4.8 $F\ cm^{-3}$ (at 20 $mV\ s^{-1}$)	2 $mW\ h\ cm^{-3}$	6.57 $W\ cm^{-3}$	1.6	100% (a cycle at 100% strain)	[160]

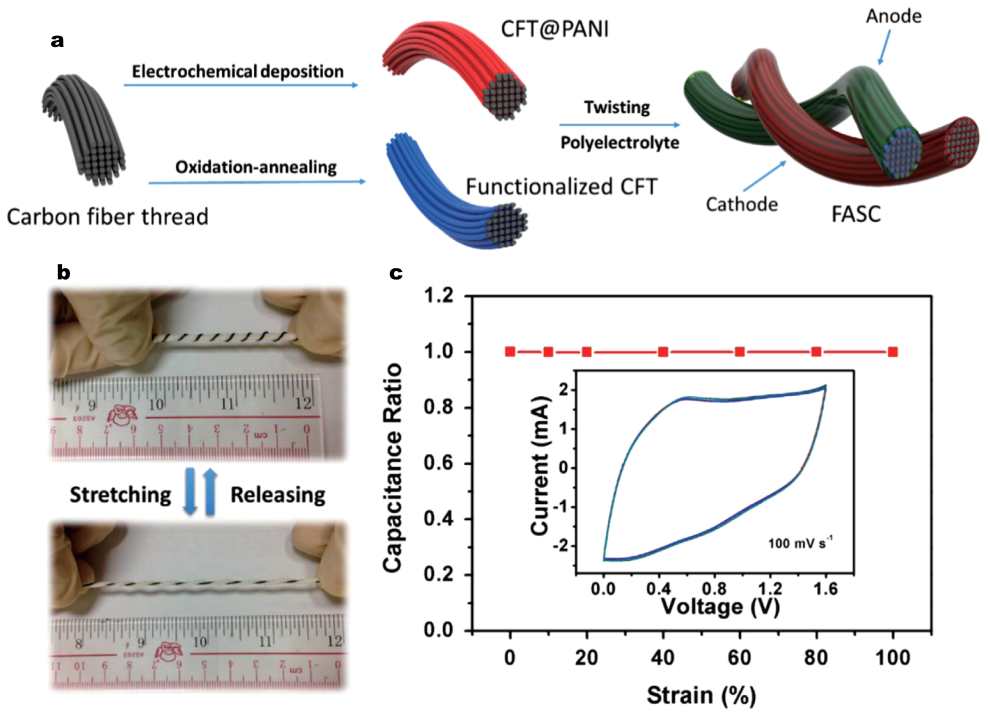

Figure 12 (a) Schematic diagram of the fabrication procedure of an SSC. (b) Digital images of the stretchable SSC before and after stretching. (c) Capacitance ratio of the SSC under different applied strains at a scan rate of 100 mV s^{-1}. Inset shows the CV curves of the SSC measured at different applied tensile strains. (Reproduced with permission from Ref. [160], Copyright 2014, Elsevier).

stance, one-dimensional wire format could be fabricated by using buckled or elastomeric electrodes with twisted or coaxial structure. Moreover the pre-existing textile was directly coated by active materials. Compared to the twisted structure, the fiber with a coaxial structure has fully taken advantage of the large surface area of materials with a much lower internal resistance and higher stability, but poorer mechanical properties.

On the other hand, fundamental understanding as well as deep insights on the coupling effects of mechanical electrochemical properties of the SSCs are emerging and the optimal combination of the targeted properties have been accomplished through different stretching mode and SC design. As far as the published work is concerned, however, the fabrication of SSC for the industrialized application and further study into the interface mechanics between nanomaterials and elastomeric substrates of SSCs should have attracted tremendous interest. Overall, accompanying with the technical breakthroughs in material production and device design, we believe that carbon-based stretchable SCs will be seen in our daily lives.

Received 28 April 2016; accepted 31 May 2016; published online 23 June 2016

1 Yao S, Zhu Y. Nanomaterial-enabled stretchable conductors: strategies, materials and devices. Adv Mater, 2015, 27: 1480–1511
2 Zhu W, Yogeesh MN, Yang S, *et al.* Flexible black phosphorus ambipolar transistors, circuits and AM demodulator. Nano Lett, 2015, 15: 1883–1890
3 Kang H, Jung S, Jeong S, *et al.* Polymer-metal hybrid transparent electrodes for flexible electronics. Nat Commun, 2015, 6: 6503
4 Wang X, Li Z, Xu W, *et al.* TiO_2 nanotube arrays based flexible perovskite solar cells with transparent carbon nanotube electrode. Nano Energy, 2015, 11: 728–735
5 Kim BJ, Kim DH, Lee YY, *et al.* Highly efficient and bending durable perovskite solar cells: toward a wearable power source. Energy Environ Sci, 2015, 8: 916–921
6 Yu R, Wu W, Ding Y, *et al.* GaN nanobelt-based strain-gated piezotronic logic devices and computation. ACS Nano, 2013, 7: 6403–6409
7 Shin G, Bae MY, Lee HJ, *et al.* SnO_2 nanowire logic devices on deformable nonplanar substrates. ACS Nano, 2011, 5: 10009–10016
8 Son D, Koo JH, Song JK, *et al.* Stretchable carbon nanotube charge-trap floating-gate memory and logic devices for wearable electronics. ACS Nano, 2015, 9: 5585–5593
9 Ho X, Cheng CK, Tan RLS, *et al.* Screen printing of stretchable electrodes for large area LED matrix. J Mater Res, 2015, 30: 2271–2278
10 Li Z, Le T, Wu Z, *et al.* Rational design of a printable, highly conductive silicone-based electrically conductive adhesive for stretchable radio-frequency antennas. Adv Funct Mater, 2015, 25: 464–470
11 Kim BS, Shin KY, Pyo JB, *et al.* Reversibly stretchable, optically transparent radio-frequency antennas based on wavy Ag nanowire networks. ACS Appl Mater Interfaces, 2016, 8: 2582–2590
12 Chiang CW, Haider G, Tan WC, *et al.* Highly stretchable and sensitive photodetectors based on hybrid graphene and graphene quan-

tum dots. ACS Appl Mater Interfaces, 2016, 8: 466–471
13 Yan C, Wang J, Wang X, *et al.* An intrinsically stretchable nanowire photodetector with a fully embedded structure. Adv Mater, 2014, 26: 943–950
14 Lee Y, Shin M, Thiyagarajan K, *et al.* Approaches to stretchable polymer active channels for deformable transistors. Macromolecules, 2016, 49: 433–444
15 Yan C, Wang J, Kang W, *et al.* Highly stretchable piezoresistive graphene-nanocellulose nanopaper for strain sensors. Adv Mater, 2014, 26: 2022–2027
16 Amjadi M, Turan M, Clementson C P, *et al.* Parallel microcracks-based ultrasensitive and highly stretchable strain sensors. ACS Appl Mater Interfaces, 2016, 8: 5618–5626
17 Trung TQ, Ramasundaram S, Hwang BU, *et al.* An all-elastomeric transparent and stretchable temperature sensor for body-attachable wearable electronics. Adv Mater, 2016, 28: 502–509
18 Hong SY, Lee YH, Park H, *et al.* Stretchable active matrix temperature sensor array of polyaniline nanofibers for electronic skin. Adv Mater, 2016, 28: 930–935
19 Zhao X, Hua Q, Yu R, *et al.* Flexible, stretchable and wearable multifunctional sensor array as artificial electronic skin for static and dynamic strain mapping. Adv Electron Mater, 2015, 1: 1500142
20 Ge J, Sun L, Zhang FR, *et al.* A stretchable electronic fabric artificial skin with pressure-, lateral strain-, and flexion-sensitive properties. Adv Mater, 2016, 28: 722–728
21 Yu Y, Zhang Y, Li K, *et al.* Bio-inspired chemical fabrication of stretchable transparent electrodes. Small, 2015, 11: 3444–3449
22 Guo Y, Li YH, Guo Z, *et al.* Bio-inspired stretchable absolute pressure sensor network. Sensors, 2016, 16: 55–66
23 Xu Y, Zhang Y, Guo Z, *et al.* Flexible, stretchable, and rechargeable fiber-shaped zinc-air battery based on cross-stacked carbon nanotube sheets. Angew Chem Int Ed, 2015, 54: 15390–15394
24 Wagner S, Bauer S. Materials for stretchable electronics. MRS Bull, 2012, 37: 207–213
25 Yoon J, Baca AJ, Park SI, *et al.* Ultrathin silicon solar microcells for semitransparent, mechanically flexible and microconcentrator module designs. Nat Mater, 2008, 7: 907–915
26 Luo Y, Luo J, Jiang J, *et al.* Seed-assisted synthesis of highly ordered TiO_2@α-Fe_2O_3 core/shell arrays on carbon textiles for lithium-ion battery applications. Energy Environ Sci, 2012, 5: 6559–6566
27 Xu S, Zhang Y, Cho J, *et al.* Stretchable batteries with self-similar serpentine interconnects and integrated wireless recharging systems. Nat Commun, 2013, 4: 1543
28 Lee J, Kim W, Kim W. Stretchable carbon nanotube/ion–gel supercapacitors with high durability realized through interfacial microroughness. ACS Appl Mater Interfaces, 2014, 6: 13578–13586
29 Zeng Y, Han Y, Zhao Y, *et al.* Advanced Ti-doped Fe_2O_3@PEDOT core/shell anode for high-energy asymmetric supercapacitors. Adv Energy Mater, 2015, 5: 1402176
30 Lu X, Yu M, Wang G, *et al.* H-TiO_2@MnO_2//H-TiO_2 @C core-shell nanowires for high performance and flexible asymmetric supercapacitors. Adv Mater, 2013, 25: 267–272
31 Feng J, Sun X, Wu C, *et al.* Metallic few-layered VS_2 ultrathin nanosheets: high two-dimensional conductivity for in-plane supercapacitors. J Am Chem Soc, 2011, 133: 17832–17838
32 Wu C, Lu X, Peng L, *et al.* Two-dimensional vanadyl phosphate ultrathin nanosheets for high energy density and flexible pseudocapacitors. Nat Commun, 2013, 4: 2431
33 Xiao X, Peng X, Jin H, *et al.* Freestanding mesoporous VN/CNT hybrid electrodes for flexible all-solid-state supercapacitors. Adv Mater, 2013, 25: 5091–5097
34 Huang Y, Tao J, Meng W, *et al.* Super-high rate stretchable polypyrrole-based supercapacitors with excellent cycling stability. Nano Energy, 2015, 11: 518–525
35 Yu M, Zhang Y, Zeng Y, *et al.* Water surface assisted synthesis of large-scale carbon nanotube film for high-performance and stretchable supercapacitors. Adv Mater, 2014, 26: 4724–4729
36 Yu G, Xie X, Pan L, *et al.* Hybrid nanostructured materials for high-performance electrochemical capacitors. Nano Energy, 2013, 2: 213–234
37 Hu L, Chen W, Xie X, *et al.* Symmetrical MnO_2–carbon nanotube–textile nanostructures for wearable pseudocapacitors with high mass loading. ACS Nano, 2011, 5: 8904–8913
38 Nyholm L, Nyström G, Mihranyan A, *et al.* Toward flexible polymer and paper-based energy storage devices. Adv Mater, 2011, 23: 3751–3769
39 Gamby J, Taberna P L, Simon P, *et al.* Studies and characterisations of various activated carbons used for carbon/carbon supercapacitors. J Power Sources, 2001, 101: 109–116
40 Frackowiak E, Béguin F. Carbon materials for the electrochemical storage of energy in capacitors. Carbon, 2001, 39: 937–950
41 Dai L, Chang DW, Baek JB, *et al.* Carbon nanomaterials for advanced energy conversion and storage. Small, 2012, 8: 1130–1166
42 Tao XY, Zhang XB, Zhang L, *et al.* Synthesis of multi-branched porous carbon nanofibers and their application in electrochemical double-layer capacitors. Carbon, 2006, 44: 1425–1428
43 Wang DW, Li F, Chen ZG, *et al.* Synthesis and electrochemical property of boron-doped mesoporous carbon in supercapacitor. Chem Mater, 2008, 20: 7195–7200
44 Candelaria SL, Uchaker E, Cao G. Comparison of surface and bulk nitrogen modification in highly porous carbon for enhanced supercapacitors. Sci China Mater, 2015, 58: 521–533
45 Futaba DN, Hata K, Yamada T, *et al.* Shape-engineerable and highly densely packed single-walled carbon nanotubes and their application as super-capacitor electrodes. Nat Mater, 2006, 5: 987–994
46 Hou PX, Song M, Li JC, *et al.* Synthesis of high quality nitrogen-doped single-wall carbon nanotubes. Sci China Mater, 2015, 58: 603–610
47 Zhang LL, Zhou R, Zhao XS. Graphene-based materials as supercapacitor electrodes. J Mater Chem, 2010, 20: 5983
48 Hou J, Shao Y, Ellis MW, *et al.* Graphene-based electrochemical energy conversion and storage: fuel cells, supercapacitors and lithium ion batteries. Phys Chem Chem Phys, 2011, 13: 15384–15402
49 Chmiola J. Anomalous increase in carbon capacitance at pore sizes less than 1 nanometer. Science, 2006, 313: 1760–1763
50 Morin SA, Bierman MJ, Tong J, *et al.* Mechanism and kinetics of spontaneous nanotube growth driven by screw dislocations. Science, 2010, 328: 476–480
51 Wang K, Zhao P, Zhou X, *et al.* Flexible supercapacitors based on cloth-supported electrodes of conducting polymer nanowire array/SWCNT composites. J Mater Chem, 2011, 21: 16373–16378
52 Wu Q, Xu Y, Yao Z, *et al.* Supercapacitors based on flexible graphene/polyaniline nanofiber composite films. ACS Nano, 2010, 4: 1963–1970
53 Cong HP, Ren XC, Wang P, *et al.* Flexible graphene–polyaniline composite paper for high-performance supercapacitor. Energy Environ Sci, 2013, 6: 1185–1191
54 Lu J, Liu W, Ling H, *et al.* Layer-by-layer assembled sulfonated-graphene/polyaniline nanocomposite films: enhanced electrical and ionic conductivities, and electrochromic properties. RSC Adv, 2012, 2: 10537–10543
55 Huang Y, Huang Y, Meng W, *et al.* Enhanced tolerance to stretch-induced performance degradation of stretchable MnO_2-based su-

percapacitors. ACS Appl Mater Interfaces, 2015, 7: 2569–2574
56 Zhao C, Wang C, Yue Z, *et al.* Intrinsically stretchable supercapacitors composed of polypyrrole electrodes and highly stretchable gel electrolyte. ACS Appl Mater Interfaces, 2013, 5: 9008–9014
57 Wu J, Zhou D, Too CO, *et al.* Conducting polymer coated lycra. Synt Metal, 2005, 155: 698–701
58 Huang Y, Li H, Wang Z, *et al.* Nanostructured polypyrrole as a flexible electrode material of supercapacitor. Nano Energy, 2016, 22: 422–438
59 Alvi F, Ram MK, Basnayaka PA, *et al.* Graphene–polyethylenedioxythiophene conducting polymer nanocomposite based supercapacitor. Electrochim Acta, 2011, 56: 9406–9412
60 Zhai T, Xie S, Yu M, *et al.* Oxygen vacancies enhancing capacitive properties of MnO_2 nanorods for wearable asymmetric supercapacitors. Nano Energy, 2014, 8: 255–263
61 Zhai T, Wang F, Yu M, *et al.* 3D MnO_2–graphene composites with large areal capacitance for high-performance asymmetric supercapacitors. Nanoscale, 2013, 5: 6790–6796
62 Luan F, Wang G, Ling Y, *et al.* High energy density asymmetric supercapacitors with a nickel oxide nanoflake cathode and a 3D reduced graphene oxide anode. Nanoscale, 2013, 5: 7984–7990
63 Yu M, Wang W, Li C, *et al.* Scalable self-growth of Ni@NiO core-shell electrode with ultrahigh capacitance and super-long cyclic stability for supercapacitors. NPG Asia Mater, 2014, 6: e129
64 Hu CC, Chang KH, Lin MC, *et al.* Design and tailoring of the nanotubular arrayed architecture of hydrous RuO_2 for next generation supercapacitors. Nano Lett, 2006, 6: 2690–2695
65 Nie Z, Wang Y, Zhang Y, *et al.* Multi-shelled α-Fe_2O_3 microspheres for high-rate supercapacitors. Sci China Mater, 2016, 59: 247–253
66 Zhai T, Lu X, Ling Y, *et al.* A new benchmark capacitance for supercapacitor anodes by mixed-valence sulfur-doped V_6O_{13-x}. Adv Mater, 2014, 26: 5869–5875
67 Lu X, Yu M, Zhai T, *et al.* High energy density asymmetric quasi-solid-state supercapacitor based on porous vanadium nitride nanowire anode. Nano Lett, 2013, 13: 2628–2633
68 Yu M, Zeng Y, Han Y, *et al.* Valence-optimized vanadium oxide supercapacitor electrodes exhibit ultrahigh capacitance and super-long cyclic durability of 100 000 cycles. Adv Funct Mater, 2015, 25: 3534–3540
69 Lu L, Zhu Y, Li F, *et al.* Carbon titania mesoporous composite whisker as stable supercapacitor electrode material. J Mater Chem, 2010, 20: 7645–7651
70 Zheng H, Zhai T, Yu M, *et al.* TiO_2@C core–shell nanowires for high-performance and flexible solid-state supercapacitors. J Mater Chem C, 2013, 1: 225–229
71 Mahmood N, Tahir M, Mahmood A, *et al.* Role of anions on structure and pseudocapacitive performance of metal double hydroxides decorated with nitrogen-doped graphene. Sci China Mater, 2015, 58: 114–125
72 Lee JH, Lee KY, Gupta MK, *et al.* Highly stretchable piezoelectric-pyroelectric hybrid nanogenerator. Adv Mater, 2014, 26: 765–769
73 Li X, Gu T, Wei B. Dynamic and galvanic stability of stretchable supercapacitors. Nano Lett, 2012, 12: 6366–6371
74 Gu T, Wei B. Fast and stable redox reactions of MnO_2/CNT hybrid electrodes for dynamically stretchable pseudocapacitors. Nanoscale, 2015, 7: 11626–11632
75 Yue B, Wang C, Ding X, *et al.* Polypyrrole coated nylon lycra fabric as stretchable electrode for supercapacitor applications. Electrochim Acta, 2012, 68: 18–24
76 Ellis BL, Knauth P, Djenizian T. Three-dimensional self-supported metal oxides for advanced energy storage. Adv Mater, 2014, 26: 3368–3397
77 Cao Z, Wei BBQ. A perspective: carbon nanotube macro-films for energy storage. Energy Environ Sci, 2013, 6: 3183–3201
78 Gadipelli S, Guo ZX. Graphene-based materials: synthesis and gas sorption, storage and separation. Prog Mater Sci, 2015, 69: 1–60
79 Faraji S, Ani FN. The development supercapacitor from activated carbon by electroless plating-a review. Renew Sust Energ Rev, 2015, 42: 823–834
80 Dutta S, Bhaumik A, Wu KCW. Hierarchically porous carbon derived from polymers and biomass: effect of interconnected pores on energy applications. Energy Environ Sci, 2014, 7: 3574–3592
81 Yu C, Masarapu C, Rong J, *et al.* Stretchable supercapacitors based on buckled single-walled carbon-nanotube macrofilms. Adv Mater, 2009, 21: 4793–4797
82 Wei BQ, Vajtai R, Jung Y, *et al.* Microfabrication technology: organized assembly of carbon nanotubes. Nature, 2002, 416: 495–496
83 Cao Q, Rogers JA. Ultrathin films of single-walled carbon nanotubes for electronics and sensors: a review of fundamental and applied aspects. Adv Mater, 2009, 21: 29–53
84 Baughman RH. Carbon nanotubes-the route toward applications. Science, 2002, 297: 787–792
85 Wei BQ, Vajtai R, Ajayan PM. Reliability and current carrying capacity of carbon nanotubes. Appl Phys Lett, 2001, 79: 1172–1174
86 Peigney A, Laurent C, Flahaut E, *et al.* Specific surface area of carbon nanotubes and bundles of carbon nanotubes. Carbon, 2001, 39: 507–514
87 Zeng S, Chen H, Cai F, *et al.* Electrochemical fabrication of carbon nanotube/polyaniline hydrogel film for all-solid-state flexible supercapacitor with high areal capacitance. J Mater Chem A, 2015, 3: 23864–23870
88 Tang Q, Chen M, Wang G, *et al.* A facile prestrain-stick-release assembly of stretchable supercapacitors based on highly stretchable and sticky hydrogel electrolyte. J Power Sources, 2015, 284: 400–408
89 Zhang N, Luan P, Zhou W, *et al.* Highly stretchable pseudocapacitors based on buckled reticulate hybrid electrodes. Nano Res, 2014, 7: 1680–1690
90 Chen T, Peng H, Durstock M, *et al.* High-performance transparent and stretchable all-solid supercapacitors based on highly aligned carbon nanotube sheets. Sci Rep, 2014, 4: 3612
91 Xu P, Kang J, Choi JB, *et al.* Laminated ultrathin chemical vapor deposition graphene films based stretchable and transparent high-rate supercapacitor. ACS Nano, 2014, 8: 9437–9445
92 Qi D, Liu Z, Liu Y, *et al.* Suspended wavy graphene microribbons for highly stretchable microsupercapacitors. Adv Mater, 2015, 27: 5559–5566
93 Chen X, Lin H, Chen P, *et al.* Smart, stretchable supercapacitors. Adv Mater, 2014, 26: 4444–4449
94 Hu L, Pasta M, Mantia FL, *et al.* Stretchable, porous, and conductive energy textiles. Nano Lett, 2010, 10: 708–714
95 Jeong HT, Kim BC, Gorkin R, *et al.* Capacitive behavior of latex/single-wall carbon nanotube stretchable electrodes. Electrochim Acta, 2014, 137: 372–380
96 Jeong HT, Kim BC, Higgins MJ, *et al.* Highly stretchable reduced graphene oxide (rGO)/single-walled carbon nanotubes (SWNTs) electrodes for energy storage devices. Electrochim Acta, 2015, 163: 149–160
97 Tang Z, Tang C, Gong H. A high energy density asymmetric supercapacitor from nano-architectured $Ni(OH)_2$/carbon nanotube electrodes. Adv Funct Mater, 2012, 22: 1272–1278
98 Huang Y, Li Y, Hu Z, *et al.* A carbon modified MnO_2 nanosheet array as a stable high-capacitance supercapacitor electrode. J Mater Chem A, 2013, 1: 9809–9813

99 Wu TM, Lin YW, Liao CS. Preparation and characterization of polyaniline/multi-walled carbon nanotube composites. Carbon, 2005, 43: 734–740
100 Chen J, Liu H, Weimer WA, *et al.* Noncovalent engineering of carbon nanotube surfaces by rigid, functional conjugated polymers. J Am Chem Soc, 2002, 124: 9034–9035
101 Tang Q, Chen M, Yang C, *et al.* Enhancing the energy density of asymmetric stretchable supercapacitor based on wrinkled CNT@MnO_2 cathode and CNT@polypyrrole anode. ACS Appl Mater Interfaces, 2015, 7: 15303–15313
102 Pasta M, La mantia F, Hu L, *et al.* Aqueous supercapacitors on conductive cotton. Nano Res, 2010, 3: 452–458
103 Bao L, Li X. Towards textile energy storage from cotton T-shirts. Adv Mater, 2012, 24: 3246–3252
104 Yun TG, Hwang B, Kim D, *et al.* Polypyrrole-MnO_2-coated textile-based flexible-stretchable supercapacitor with high electrochemical and mechanical reliability. ACS Appl Mater Interfaces, 2015, 7: 9228–9234
105 Huang Y, Zhong M, Huang Y, *et al.* A self-healable and highly stretchable supercapacitor based on a dual crosslinked polyelectrolyte. Nat Commun, 2015, 6: 10310
106 Hong SY, Yoon J, Jin SW, *et al.* High-density, stretchable, all-solid-state microsupercapacitor arrays. ACS Nano, 2014, 8: 8844–8855
107 Nam I, Kim GP, Park S, *et al.* Fabrication and design equation of film-type large-scale interdigitated supercapacitor chips. Nanoscale, 2012, 4: 7350–7353
108 Jiang H, Khang DY, Song J, *et al.* Finite deformation mechanics in buckled thin films on compliant supports. Proc Natl Acad Sci USA, 2007, 104: 15607–15612
109 Pech D, Brunet M, Durou H, *et al.* Ultrahigh-power micrometre-sized supercapacitors based on onion-like carbon. Nat Nanotech, 2010, 5: 651–654
110 Kim D, Shin G, Kang YJ, *et al.* Fabrication of a stretchable solid-state micro-supercapacitor array. ACS Nano, 2013, 7: 7975–7982
111 Yang Z, Deng J, Chen X, *et al.* A highly stretchable, fiber-shaped supercapacitor. Angew Chem Int Ed, 2013, 52: 13453–13457
112 Chen T, Hao R, Peng H, *et al.* High-performance, stretchable, wire-shaped supercapacitors. Angew Chem Int Ed, 2015, 54: 618–622
113 Xu P, Gu T, Cao Z, *et al.* Carbon nanotube fiber based stretchable wire-shaped supercapacitors. Adv Energy Mater, 2014, 4: 1300759
114 Choi C, Kim SH, Sim HJ, *et al.* Stretchable, weavable coiled carbon nanotube/MnO_2/polymer fiber solid-state supercapacitors. Sci Rep, 2015, 5: 9387
115 Zhang Y, Bai W, Cheng X, *et al.* Flexible and stretchable lithium-ion batteries and supercapacitors based on electrically conducting carbon nanotube fiber springs. Angew Chem Int Ed, 2014, 53: 14564–14568
116 Xu P, Wei B, Cao Z, *et al.* Stretchable wire-shaped asymmetric supercapacitors based on pristine and MnO_2 coated carbon nanotube fibers. ACS Nano, 2015, 9: 6088–6096
117 Shang Y, Wang C, He X, *et al.* Self-stretchable, helical carbon nanotube yarn supercapacitors with stable performance under extreme deformation conditions. Nano Energy, 2015, 12: 401–409
118 Chen X, Qiu L, Ren J, *et al.* Novel electric double-layer capacitor with a coaxial fiber structure. Adv Mater, 2013, 25: 6436–6441
119 Zhang N, Zhou W, Zhang Q, *et al.* Biaxially stretchable supercapacitors based on the buckled hybrid fiber electrode array. Nanoscale, 2015, 7: 12492–12497
120 Novoselov KS. Electric field effect in atomically thin carbon films. Science, 2004, 306: 666–669
121 Yu C, Liu Z, Chen Y, *et al.* CoS nanosheets-coupled graphene quantum dots architectures as a binder-free counter electrode for high-performance DSSCs. Sci China Mater, 2016, 59: 104–111
122 Balandin AA, Ghosh S, Bao W, *et al.* Superior thermal conductivity of single-layer graphene. Nano Lett, 2008, 8: 902–907
123 Wang DW, Li F. Porous yet dense metal-free electro-materials for compact energy storage. Sci China Mater, 2016, 59: 4–5
124 King A, Johnson G, Engelberg D, *et al.* Observations of intergranular stress corrosion cracking in a grain-mapped polycrystal. Science, 2008, 321: 382–385
125 Zhao H, Jiao T, Zhang L, *et al.* Preparation and adsorption capacity evaluation of graphene oxide-chitosan composite hydrogels. Sci China Mater, 2015, 58: 811–818
126 Zhu Y, Murali S, Stoller MD, *et al.* Carbon-based supercapacitors produced by activation of graphene. Science, 2011, 332: 1537–1541
127 Stankovich S, Dikin DA, Dommett GHB, *et al.* Graphene-based composite materials. Nature, 2006, 442: 282–286
128 Wang Z, Jia W, Jiang M, *et al.* Microwave-assisted synthesis of layer-by-layer ultra-large and thin NiAl-LDH/RGO nanocomposites and their excellent performance as electrodes. Sci China Mater, 2015, 58: 944–952
129 Zheng H, Smith RK, Jun Y, *et al.* Observation of single colloidal platinum nanocrystal growth trajectories. Science, 2009, 324: 1309–1312
130 Yu D, Dai L. Self-assembled graphene/carbon nanotube hybrid films for supercapacitors. J Phys Chem Lett, 2010, 1: 467–470
131 Wang X, Shi G. Flexible graphene devices related to energy conversion and storage. Energy Environ Sci, 2015, 8: 790–823
132 Sheng K, Sun Y, Li C, *et al.* Ultrahigh-rate supercapacitors based on eletrochemically reduced graphene oxide for ac line-filtering. Sci Rep, 2012, 2: 247
133 Wang W, Guo S, Penchev M, *et al.* Three dimensional few layer graphene and carbon nanotube foam architectures for high fidelity supercapacitors. Nano Energy, 2013, 2: 294–303
134 Chen Z, Ren W, Gao L, *et al.* Three-dimensional flexible and conductive interconnected graphene networks grown by chemical vapour deposition. Nat Mater, 2011, 10: 424–428
135 Li F, Chen J, Wang X, *et al.* Stretchable supercapacitor with adjustable volumetric capacitance based on 3D interdigital electrodes. Adv Funct Mater, 2015, 25: 4601–4606
136 Xie Y, Liu Y, Zhao Y, *et al.* Stretchable all-solid-state supercapacitor with wavy shaped polyaniline/graphene electrode. J Mater Chem A, 2014, 2: 9142–9149
137 Peng L, Peng X, Liu B, *et al.* Ultrathin two-dimensional MnO_2/graphene hybrid nanostructures for high-performance, flexible planar supercapacitors. Nano Lett, 2013, 13: 2151–2157
138 Nam I, Bae S, Park S, *et al.* Omnidirectionally stretchable, high performance supercapacitors based on a graphene-carbon-nanotube layered structure. Nano Energy, 2015, 15: 33–42
139 Basnayaka PA, Ram MK, Stefanakos L, *et al.* High performance graphene-poly (o-anisidine) nanocomposite for supercapacitor applications. Mater Chem Phys, 2013, 141: 263–271
140 Tamilarasan P, Ramaprabhu S. Stretchable supercapacitors based on highly stretchable ionic liquid incorporated polymer electrolyte. Mater Chem Phys, 2014, 148: 48–56
141 Chen T, Xue Y, Roy AK, *et al.* Transparent and stretchable high-performance supercapacitors based on wrinkled graphene electrodes. ACS Nano, 2014, 8: 1039–1046
142 Xu P, Kang J, Suhr J, *et al.* Spatial strain variation of graphene films for stretchable electrodes. Carbon, 2015, 93: 620–624
143 Zang J, Cao C, Feng Y, *et al.* Stretchable and high-performance supercapacitors with crumpled graphene papers. Sci Rep, 2014, 4: 6492
144 Dong Z, Jiang C, Cheng H, *et al.* Facile fabrication of light, flex-

ible and multifunctional graphene fibers. Adv Mater, 2012, 24: 1856–1861
145 Xu Z, Gao C. Graphene chiral liquid crystals and macroscopic assembled fibres. Nat Commun, 2011, 2: 571
146 Cong H P, Ren X C, Wang P, *et al.* Wet-spinning assembly of continuous, neat, and macroscopic graphene fibers. Sci Rep, 2012, 2: 613
147 Yu G, Hu L, Vosgueritchian M, *et al.* Solution-processed graphene/MnO_2 nanostructured textiles for high-performance electrochemical capacitors. Nano Lett, 2011, 11: 2905–2911
148 Wang Y, Peng Y, Wang D, *et al.* Wet deposition fluxes of total mercury and methylmercury in core urban areas, Chongqing, China. Atmos Environ, 2014, 92: 87–96
149 Liu W, Yan X, Lang J, *et al.* Flexible and conductive nanocomposite electrode based on graphene sheets and cotton cloth for supercapacitor. J Mater Chem, 2012, 22: 17245–17253
150 Carretero-González J, Castillo-martínez E, Dias-lima M, *et al.* Oriented graphene nanoribbon yarn and sheet from aligned multiwalled carbon nanotube sheets. Adv Mater, 2012, 24: 5695–5701
151 Kou L, Huang T, Zheng B, *et al.* Coaxial wet-spun yarn supercapacitors for high-energy density and safe wearable electronics. Nat Commun, 2014, 5: 3754
152 Yu D, Goh K, Wang H, *et al.* Scalable synthesis of hierarchically structured carbon nanotube–graphene fibres for capacitive energy storage. Nat Nanotech, 2014, 9: 555–562
153 Tao J, Liu N, Ma W, *et al.* Solid-state high performance flexible supercapacitors based on polypyrrole-MnO_2-carbon fiber hybrid structure. Sci Rep, 2013, 3: 2286
154 Lee J A, Shin M K, Kim S H, *et al.* Ultrafast charge and discharge biscrolled yarn supercapacitors for textiles and microdevices. Nat Commun, 2013, 4: 1970
155 Huang Y, Hu H, Huang Y, *et al.* From industrially weavable and knittable highly conductive yarns to large wearable energy storage textiles. ACS Nano, 2015, 9: 4766–4775
156 Meng Y, Zhao Y, Hu C, *et al.* All-graphene core-sheath microfibers for all-solid-state, stretchable fibriform supercapacitors and wearable electronic textiles. Adv Mater, 2013, 25: 2326–2331
157 Zang X, Zhu M, Li X, *et al.* Dynamically stretchable supercapacitors based on graphene woven fabric electrodes. Nano Energy, 2015, 15: 83–91
158 Zhao C, Shu K, Wang C, *et al.* Reduced graphene oxide and polypyrrole/reduced graphene oxide composite coated stretchable fabric electrodes for supercapacitor application. Electrochim Acta, 2015, 172: 12–19
159 Zhao Y, Liu J, Hu Y, *et al.* Highly compression-tolerant supercapacitor based on polypyrrole-mediated graphene foam electrodes. Adv Mater, 2013, 25: 591–595
160 Jin H, Zhou L, Mak CL, *et al.* High-performance fiber-shaped supercapacitors using carbon fiber thread (CFT)@polyanilne and functionalized CFT electrodes for wearable/stretchable electronics. Nano Energy, 2015, 11: 662–670
161 Yan X, Tai Z, Chen J, *et al.* Fabrication of carbon nanofiber–polyaniline composite flexible paper for supercapacitor. Nanoscale, 2011, 3: 212–216
162 Xu B, Wu F, Chen R, *et al.* Mesoporous activated carbon fiber as electrode material for high-performance electrochemical double layer capacitors with ionic liquid electrolyte. J Power Sources, 2010, 195: 2118–2124
163 Deng F, Yu L, Cheng G, *et al.* Synthesis of ultrathin mesoporous $NiCo_2O_4$ nanosheets on carbon fiber paper as integrated high-performance electrodes for supercapacitors. J Power Sources, 2014, 251: 202–207
164 Yu J, Wang L, Lai X, *et al.* A durability study of carbon nanotube fiber based stretchable electronic devices under cyclic deformation. Carbon, 2015, 94: 352–361

Acknowledgments This work was supported by the National Natural Science Foundation of China (21403306, 2141101037 and 21273290), Guangdong Natural Science Funds for Distinguished Young Scholar (2014A030306048), and the Natural Science Foundation of Guangdong Province (2014B010123002, 2014B050505001, 2015B010118002 and 2015B090927007).

Author contributions Zhang X and Yu M wrote the paper; Zhang H and Lin Z prepared all the figures and references; Lu X and Tong Y provided the overall concept and revised manuscript. All authors contributed to the general discussion.

Conflict of interest The authors declare that they have no conflict of interest.

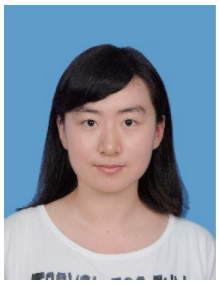

Xiyue Zhang is currently an undergraduate student in the School of Chemistry and Chemical Engineering at Sun Yat-Sen University. She joined Prof. Lu's group in 2012. Her current research focuses on the design of metal oxide nanomaterials hybrid with graphene/partially exfoliated carbon nanotube and their application in energy storage.

Xihong Lu is currently an associate professor in the School of Chemistry and Chemical Engineering at Sun Yat-Sen University, China. He received his BSc degree in applied chemistry and PhD degree in physical chemistry from Sun Yat-Sen University in 2008 and 2013, respectively. His current research focuses on the design and synthesis of functionally nanostructured materials for applications in energy conversion and storage, such as supercapacitors, Li ion batteries and photoelectrochemical/photocatalytic water splitting.

Yexiang Tong is currently a professor in the School of Chemistry and Chemical Engineering at Sun Yat-Sen University, China. He received his BSc degree in general chemistry in 1985, MSc degree in physical chemistry in 1988, and PhD in organic chemistry in 1999 from Sun Yat-Sen University. He joined Sun Yat-Sen University as an assistant professor of chemistry in 1988. His current research focuses on the electrochemical synthesis of alloys, intermetallic compounds and metal oxide nanomaterials, and investigation of their applications for energy conversion and storage.

基于碳材料的可伸缩型超级电容器的研究进展

张熙悦, 张昊喆, 林子琦, 于明浩, 卢锡洪*, 童叶翔*

摘要 可伸缩型储能器件的研究对现代电子产品的发展至关重要. 可伸缩型超级电容器(SSCs)能在大的应力应变条件下保持其储能性能不受损害, 是近年来发展的一种新型、高效、实用的储能装置. 碳纳米管和石墨烯等碳材料由于具有较大的比表面积、优良的导电性和机械性能优势, 以及突出的电化学性能, 成为伸缩型超级电容器电极材料的新选择. 近年来, 为进一步提高碳基可伸缩型超级电容器的性能, 许多课题组致力于其一维线状、二维平面/网状和三维立体结构的探索研究中. 本篇综述总结了近年来碳基可伸缩型超级电容器的研究策略和方法, 并通过分析讨论该新兴领域的一些重要挑战, 提出未来可行的研究方向.